Dynamics and facies model of a macrotidal sand-bar complex, Cobequid Bay–Salmon River Estuary (Bay of Fundy)

Article *in* Sedimentology · June 2006

DOI: 10.1111/j.1365-3091.1990.tb00624.x

CITATIONS
165

READS
171

4 authors, including:

Robert W Dalrymple
Queen's University
164 PUBLICATIONS **10,900** CITATIONS

SEE PROFILE

Brian Zaitlin
Zaitlin Geoconsulting Ltd
33 PUBLICATIONS **3,554** CITATIONS

SEE PROFILE

Sedimentology (1990) **37**, 577–612

Dynamics and facies model of a macrotidal sand-bar complex, Cobequid Bay–Salmon River Estuary (Bay of Fundy)

ROBERT W. DALRYMPLE

Department of Geological Sciences, Queen's University, Kingston, Ontario, Canada, K7L 3N6

R. JOHN KNIGHT

Petro-Canada Inc., 150, 6th Avenue S.W., Calgary, Alberta, Canada, T2P 3E3

BRIAN A. ZAITLIN

Esso Resources Canada Ltd, 237, 4th Avenue S.W., Calgary, Alberta, Canada, T2P 0H6

GERARD V. MIDDLETON

Department of Geology, McMaster University, Hamilton, Ontario, Canada, L8S 4M1

ABSTRACT

The 40-km-long, Cobequid Bay–Salmon River estuary has a maximum tidal range of 16·3 m and experiences limited wave action. Sediment, which is derived primarily from areas seaward of the estuary, is accumulating faster than the high-tide elevation is rising, and the system is progradational. The deposits consist of an axial belt of sands, which is flanked by mudflats and salt marshes in the inner half of the estuary where a funnel-shaped geometry is developed, and by erosional or non-depositional foreshores in the outer half where the system is confined by the valley walls. The axial sands are divisible into three facies zones: *zone 1*—elongate, tidal sand bars at the seaward end; *zone 2*—sand flats with a braided channel pattern; *zone 3*—the inner, single-channel, tidal–fluvial transition. Tidal current speeds reach a maximum in zone 2, but grain sizes decrease headward (from medium and coarse sand in zone 1, to fine and very fine sand in zones 2 and 3) because the headward termination of the major flood channels prevents the coarse, traction population from entering the inner part of the estuary.

Longitudinal progradation will produce a 20-m-thick, upward-fining succession, the lower ½–⅔ of which will consist of cross-bedded, medium to coarse sand deposited on the zone 1 sand bars. The ebb-dominated portion of this unit will be finer grained than the flood-dominated part, and will contain trough cross-bedding produced by 3-D megaripples; the flood-dominated areas, by contrast, will consist mainly of compound cross-bedding created by sandwaves with superimposed megaripples. Headward migration of swatchways (oblique channels that link the ebb- and flood-dominated areas) will create packages of ebb cross-bedding that is orientated at a high angle to the long axis of the estuary and that contains headward-inclined, lateral-accretion surfaces. The overlying fine and very fine sands of zones 2 and 3 will be composed mainly of upper-flow-regime parallel lamination. The succession will be capped by a 4-m-thick unit of mixed flat, mudflat and salt marsh sediments. A review of other macrotidal estuaries with tidal ranges greater than 10 m suggests that the major elements of the model have general applicability.

INTRODUCTION

It has been estimated that nearly one-third of the world's coastline is macrotidal (>4 m; Davies, 1964), and more than 10 separate areas, many of which are estuarine in character, have tidal ranges that are greater than 10 m. Based on those macrotidal estuaries for which adequate data exist [the Bristol Channel and Severn River, England (Parker & Kirby, 1982; Harris & Collins, 1985; Allen & Rae, 1988); Mont

Saint-Michel Bay, France (Larsonneur, 1975, 1988); Cook Inlet, Alaska (Bartsch-Winkler & Ovenshine, 1984; Bartsch-Winkler, 1988); South Alligator River, Australia (Woodroffe *et al.*, 1985a, b, 1989); Avon River, Cumberland Basin and Cobequid Bay–Salmon River, Bay of Fundy (Lambiase, 1977, 1980b; Amos & Long, 1980; Dalrymple, Amos & McCann, 1982; Amos & Zaitlin, 1985)], it is clear that such areas are sites of active deposition, with large volumes of sediment transported *landwards* to accumulate in shallow subtidal and intertidal settings at the head of the embayment.

Despite the abundance and depositional character of modern macrotidal estuaries, documented ancient examples are rare (Clifton, 1982; Galloway & Hobday, 1983). It seems unlikely that this scarcity reflects their true abundance, because the repeated transgression of the continents (e.g. Vail, Mitchum & Thompson, 1977) is certain to have duplicated the conditions necessary for large tidal amplification at many times and in many places. Furthermore, such estuarine deposits fill palaeo-valleys where preservation potention should be good. It is concluded that the small number of identified ancient examples reflects the failure to recognize them. All of the existing facies models for macrotidal environments (Knight & Dalrymple, 1975; Coleman & Wright, 1975; Galloway & Hobday, 1983; Harris, 1988; Terwindt, 1988) are highly schematic, and lack the detail needed for confident application to the rock record.

It is for these reasons that we present a detailed and comprehensive overview of the Cobequid Bay–Salmon River estuary (Fig. 1), and from this develop a more detailed facies model for such systems. This area is one of the most intensely studied macrotidal estuaries, but previous work (e.g. Dalrymple, Knight & Middleton, 1975; Knight & Dalrymple, 1975; Dalrymple, Knight & Lambiase, 1978; Knight, 1980; Risk & Yeo, 1980; Yeo & Risk, 1981; Dalrymple, 1984a) has generally been narrowly focused. In this paper, we describe the setting of the entire system and then focus on the elongate tidal sand bars which characterize the seaward portion of most macrotidal environments (Hayes, 1975; Harris, 1988). Other components of the system will be discussed in subsequent papers.

The nomenclature of the large-scale bedforms which are abundant in this area is the subject of considerable confusion. A new, consensus terminology has been proposed (Ashley *et al.*, 1990), but for continuity, the terminology used in previous papers (Dalrymple *et al.*, 1978; Dalrymple, 1984a) is followed. Where appropriate, the new synonyms are provided, and the term 'dune' is used to refer collectively to both megaripples and sandwaves, as advocated by Ashley *et al.* (1990).

GEOMORPHOLOGY AND GENERAL FACIES DISTRIBUTION

The study area occupies the headward portion of the eastern arm of the Bay of Fundy, and consists of Cobequid Bay and the tidally influenced portion of the Salmon River (Figs 1C & 2). Sands and/or gravels are present along the axis of the estuary, and pass laterally into either muddy, fringing facies (mixed flats, mudflats and salt marsh) or an erosional foreshore (Fig. 2). The axial sands and gravels can be subdivided into five facies zones on the basis of channel and bar-form geometry, sediment texture and bedform type (Dalrymple & Zaitlin, 1985, 1989; Zaitlin & Dalrymple, 1985a, b; Zaitlin, 1987). From seaward to landward these are (Figs 1 & 2): *zone 0*—the (generally) non-depositional, subtidal floor of the Minas Basin and outer Cobequid Bay; *zone 1*—tidal sand-bar complex (23–40 km seaward of the tidal limit) with abundant dunes; *zone 2*—upper-flow-regime sandflats (12–23 km); *zone 3*—the tidally influenced fluvial channel (0–12 km); *zone 4*—the fluvial reach above the limit of tidal influence. Together zones 1, 2 and 3 and their fringing facies constitute what is here termed the Cobequid Bay–Salmon River (CB–SR) estuarine complex (Fig. 2).

The bankfull width at mean high tide in zones 2 and 3 displays the exponential seaward increase (Fig. 3A) which typifies most tidal systems (Pillsbury, 1939; Langbein *in* Myrick & Leopold, 1963; Wright, Coleman & Thom, 1973), and the lateral extent of the axial sand facies shows a similar pattern (Fig. 3B). By contrast, the bankfull and sand facies widths are nearly constant through zone 1 (Fig. 3A, B). The break in slope of these two relationships at approximately 20 km seaward of the tidal limit occurs because the bankfull width increases at a faster rate than the valley width so that the high-tide shoreline intersects the valley walls at this point (Fig. 3A, B). Thus, the lateral extent of the complex would be greater in the outer part if the valley width permitted.

This change in the geometry at the 20-km point is clearly reflected in the nature of the fringing facies. Along the margins of zones 0 and 1, the shoreline consists of actively eroding cliffs which are fronted by erosional or non-depositional foreshores (Knight &

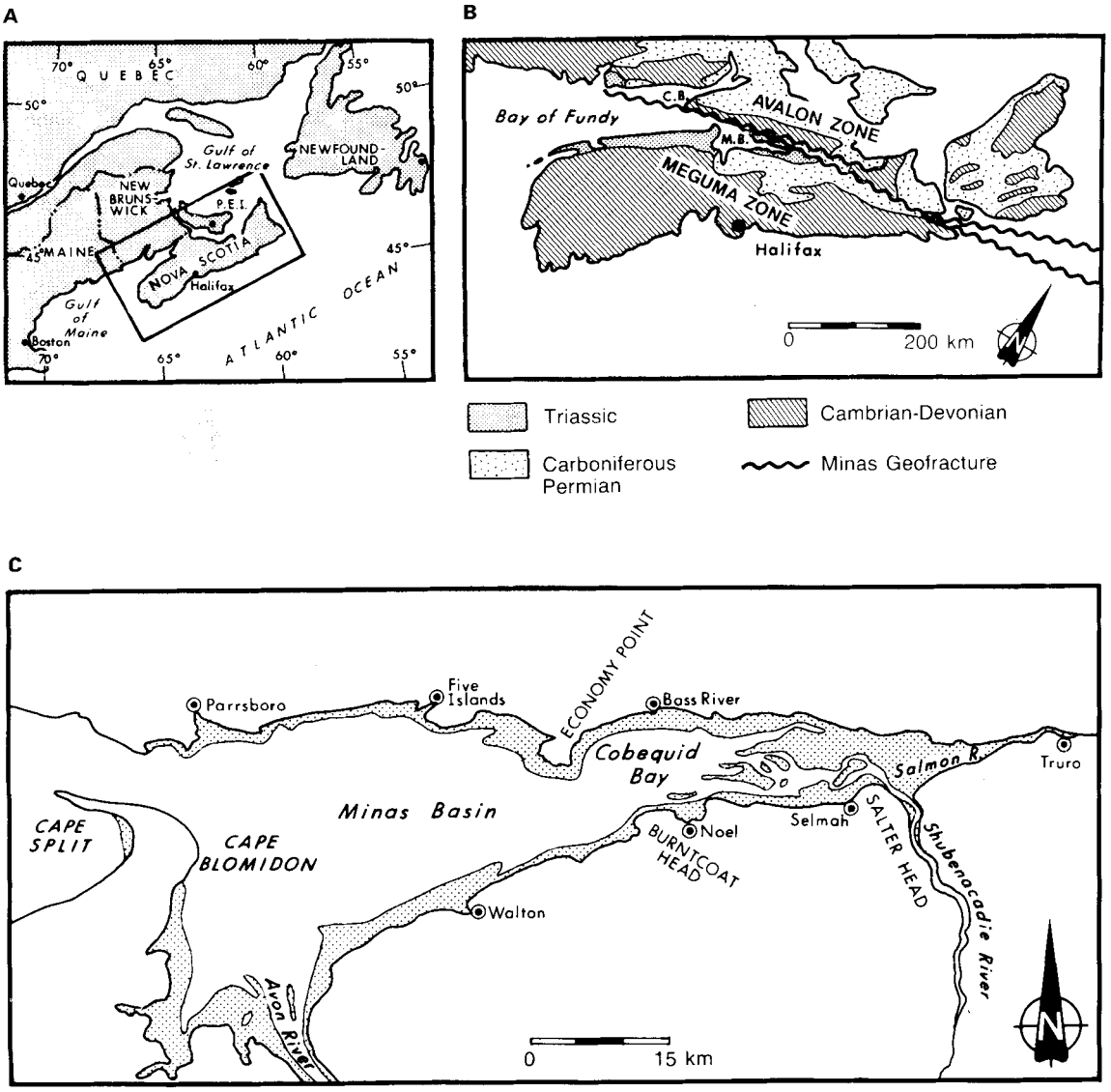

Fig. 1. (A) Location map of eastern Canada (inset shows location of B). (B) Geological map of the Bay of Fundy region (after Bujak & Donohoe, 1980). C.B.–Chignecto Bay, M.B.–Minas Basin. (C) Location map of the Minas Basin–Cobequid Bay area. Stipple shows the intertidal zone (after Knight, 1980, Fig. 10.1A).

Dalrymple, 1975; Amos & Long, 1980). Only in sheltered areas within small stream valleys do thick accumulations of mudflat and salt marsh occur (Figs 2 & 3B). As a result, sands are the predominant sediment type seaward of the 20-km point (Fig. 3C). By contrast, the fringing zone becomes depositional in character east of Salter Head because space exists between the axial sands and the valley walls for the accumulation of mixed flats, mudflats and salt marsh (Figs 2 & 3; Zaitlin, 1987). Consequently, the proportion of muddy sediments increases headward at the expense of the sandy facies (Fig. 3C).

GEOLOGICAL SETTING

The Minas Basin and Cobequid Bay occupy a structurally controlled basin that straddles the Minas

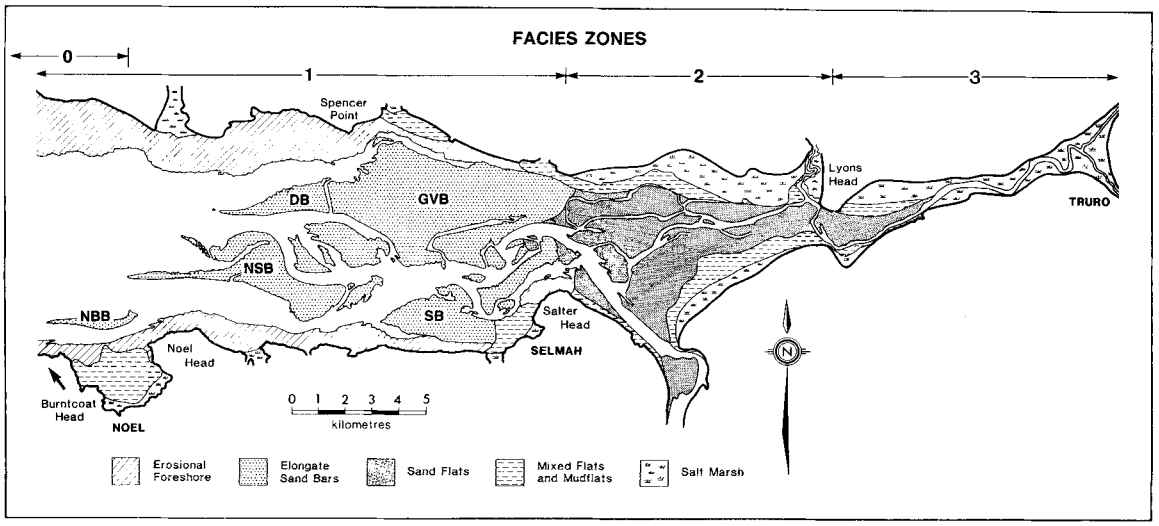

Fig. 2. Distribution of facies and facies zones in the Cobequid Bay–Salmon River estuary (after Dalrymple, Knight & Middleton, 1985). The non-depositional, subtidal zone 0 lies to the west of the zone-1 sand bars. The tidal limit, the boundary between zones 3 and 4, is located at the right-hand margin of the map. NBB–Noel Bay Bar, NSB–Noel Shore Bar, DB–Diamond Bar, GVB–Great Village Bar, SB–Selmah Bar. The bar outlines are those which existed in 1973.

geofracture (Keppie, 1982), a complex and long-lived fault system which marks the suture between the Meguma and Avalon structural zones of the Palaeozoic Appalachian orogen (Fig. 1B; Williams, 1979). During the opening of the Atlantic Ocean in the latest Triassic and earliest Jurassic, these faults were reactivated forming an asymmetrical rift valley, in which 700 m of dominantly sandy, terrestrial sediments and up to 300 m of tholeiitic basalt accumulated (Hubert & Mertz, 1980; Stevens, 1980). These basalts form Capes Blomidon and Split which isolate the Minas Basin from the main Bay of Fundy (Fig. 1B, C). The present Minas Basin–Cobequid Bay depression is believed to have been formed by Tertiary(?) fluvial action and/or Pleistocene glacial erosion which preferentially excavated the weakly consolidated Triassic sediments (Swift & Lyall, 1968; Roland, 1982).

The study area has had a complex post-glacial history which has strongly influenced the development of the estuary. During deglaciation approximately 14 000–15 000 yr BP (Amos, 1978; Grant, 1985), sea-level was up to 22 m above its present elevation (Wightman & Cooke, 1978; Fig. 4), and a series of glacio-marine deltas composed of sand and gravel was formed along the north coast of the Minas Basin and Cobequid Bay (Swift & Borns, 1967; Wightman, 1980), and in the Salmon River valley at Truro (Hennigar, 1972). Microtidal (< 2-m range) conditions prevailed at this time (Wightman, 1980). After 14 000 yr BP, sea-level fell rapidly (Fig. 4), reaching a low stand 8–13 m below present at approximately 7000 yr BP (Amos, 1978; Scott & Greenberg, 1983; Amos & Zaitlin, 1985). During this low stand, tidal ranges were mesotidal (2–4 m) as indicated by both geological evidence (Amos, 1978; Amos *et al.*, 1980; Amos & Zaitlin, 1985; R. Dalrymple, unpublished data) and computer modelling (Scott & Greenberg, 1983). Since then, mean sea-level has risen steadily at a rate of 1–1·5 mm yr^{-1} (Scott & Greenberg, 1983; Amos & Zaitlin, 1985; Bleakney, 1985). At the same time, there has been a progressive approach to resonance with the lunar semidiurnal (M_2) tide. Macrotidal conditions have existed since 4000–5000 yr BP (Fig. 4), and the tidal range continues to grow by nearly 3% per 1000 years (Scott & Greenberg, 1983). Because of the combined influence of sea-level rise and tidal amplification, the high-tide level has risen at a rate exceeding 2 mm yr^{-1} over the last 4000 years.

ENVIRONMENTAL CONDITIONS AND SEDIMENT INPUT

Tides and tidal currents

The present tidal range in the study area averages 11·9 m at Burntcoat Head (Fig. 1C; Canadian

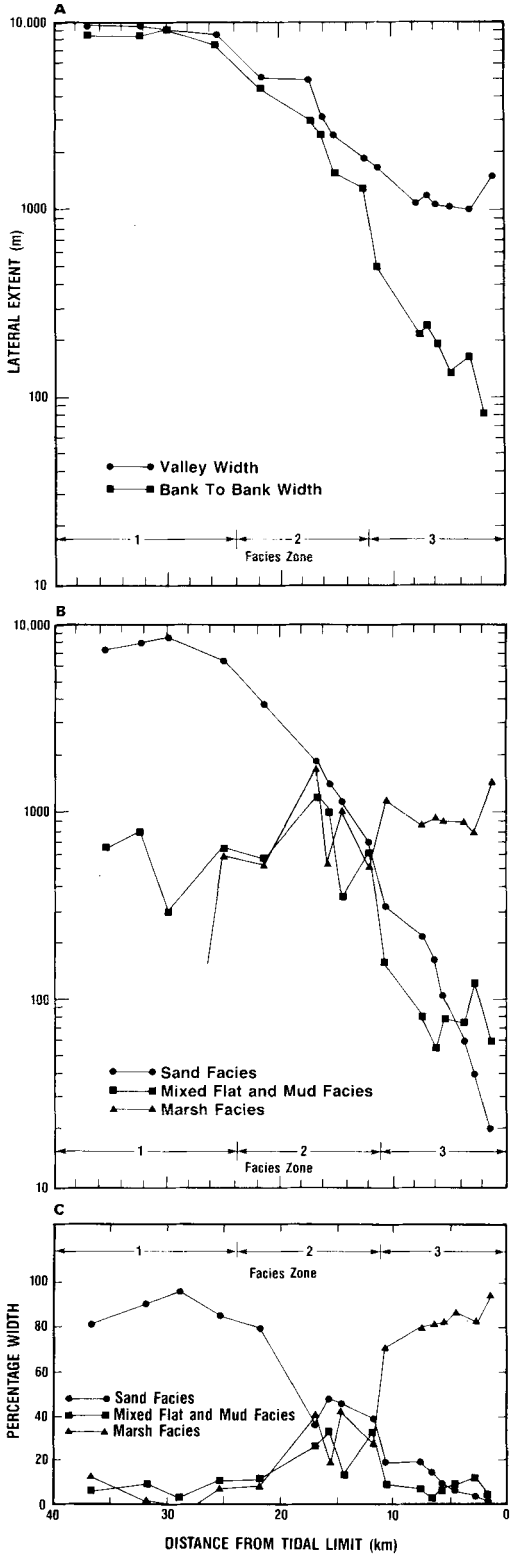

Hydrographic Service, 1984), with a maximum recorded value of 16·3 m (Dawson, 1917; Greenberg, 1979). The difference between the neap and spring tidal ranges is correspondingly large, reaching 6·5 m. In the outer Bay of Fundy (Fig. 1), the tide is a symmetrical, standing wave, but in the shallow water of Cobequid Bay it becomes modified to an asymmetrical progressive wave (Swift & McMullen, 1968; Amos & Long, 1980; Knight, 1980). This, in turn, becomes a tidal bore in the channel of the Salmon River. In the outer part of zone 1, the maximum ebb and flood current speeds are nearly equal or show a slight flood dominance, with values of approximately 1 ms^{-1} (Fig. 5). In zone 2, the average speeds of both ebb and flood currents increase dramatically to 2–3 ms^{-1}, but they then decrease gradually toward the limit of tidal influence. Thus, this estuary, like most others that are funnel-shaped, is hypersynchronous (Salomon & Allen, 1983; Nichols & Biggs, 1985). As a result of the progressive deformation of the tidal wave, and the 'truncation' of the low-water portion of the tidal curve by the landward-rising bed (Lincoln & Fitzgerald, 1988), the duration of the flood tide decreases and its current speeds increase relative to those of the ebb tide. Consequently, flood-current speeds exceed those of the ebb (on average) throughout most of the estuary, with the difference increasing headward (Fig. 5).

Waves

Due to the protective influence of Capes Blomidon and Split (Fig. 1C), all waves in the study area are locally generated. Amos & Long (1980) found that the monthly-mean, significant wave heights in the Minas Basin vary from about 0·15 to 0·6 m, with peak periods rarely exceeding 3 s. Qualitative observations indicate that the wave heights are even smaller in Cobequid Bay because this area is sheltered from the prevailing westerly winds by headlands and sand bars. In addition, the large tidal range disperses the wave energy over a wide area; therefore, the study area is overwhelmingly tide dominated (Hayes, 1979).

Fig. 3. (A) Valley width (inclusive of all modern tidal sediments) and bank-to-bank width (at the mean high-water elevation) as a function of distance from the tidal limit (after Zaitlin, 1987, Fig. 3.3). (B) and (C) Lateral extent of individual facies along the length of the estuary (after Zaitlin, 1987, Figs 3.9–3.11) expressed in terms of (B) metres and (C) percent of the valley width. Facies zones as shown in Fig. 2.

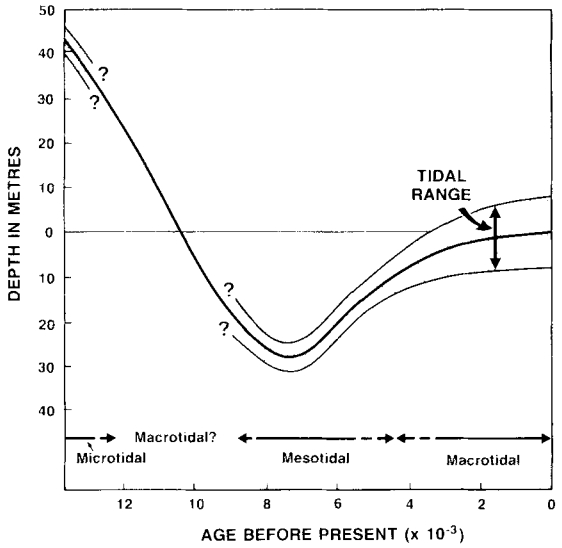

Fig. 4. History of sea-level and tidal range in Chignecto Bay (Fig. 1B; after Amos & Zaitlin, 1985). A similar pattern of sea-level variations, but with lesser amplitudes, occurred in the Minas Basin and Cobequid Bay. See test for elevations relevant to the study area.

Water characteristics

The strong tidal currents ensure that the water column is well mixed, both laterally and vertically, with respect to salinity, water temperature and suspended sediment content (Dalrymple, 1977; Knight, 1977, 1980; Amos & Long, 1980). Pronounced longitudinal gradients are evident in all of these parameters, however, and produce significant temporal variations over a tidal cycle at any point as the water mass moves in and out of the estuary. These variations are not considered further here.

The discharge of the Salmon River is low throughout most of the year (mean annual discharge approximately 10 $m^3 s^{-1}$), with a maximum of only 55–60 $m^3 s^{-1}$ in March and April (ATPEMC, 1969). The mean discharge is sufficient, however, to depress the salinity at high tide to less than 1‰ for a distance of 3 km below the tidal limit (Fig. 6; Zaitlin, 1987). From this point, the salinity rises rapidly to 20‰ in zone 2, and then more slowly to 28–29‰ at the outer end of zone 1 (ATPEMC, 1969; Amos & Long, 1980). The lack of vertical and lateral salinity gradients means that the system is a Type-C estuary in the terminology of Pritchard & Carter (1971).

In general, the shallow water at the head of the estuary is warmer in summer and cooler in winter than the deeper water of the Minas Basin. Seasonal variations are extreme everywhere, however, with values ranging from 20°C in late summer, to −0·5°C in winter (December to April) when large amounts of ice are present. This ice takes four forms (Knight & Dalrymple, 1976; Zaitlin, 1987): (i) a shore-fast ice foot at the high-tide level along the margins of zones 0, 1 and 2; (ii) loose blocks and cakes of drift ice which may cover up to 90% of the Minas Basin and Cobequid Bay (ATPEMC, 1969); (iii) a 50–500-mm-thick, accretionary ice crust which mantles most intertidal surfaces in zones 1 and 2; (iv) an unbroken ice sheet that covers the tidal reach of the Salmon River (zone 3) where the current speeds and salinity are reduced.

The suspended sediment concentration (SSC) in the Minas Basin is generally less than 5 mg l^{-1} although higher values do occur immediately after ice breakup and periods of strong wave action (Amos & Alfoldi, 1979; Greenberg & Amos, 1983). These studies also show that the SSC within Cobequid Bay increases headward to values greater than 200 mg l^{-1}; indeed,

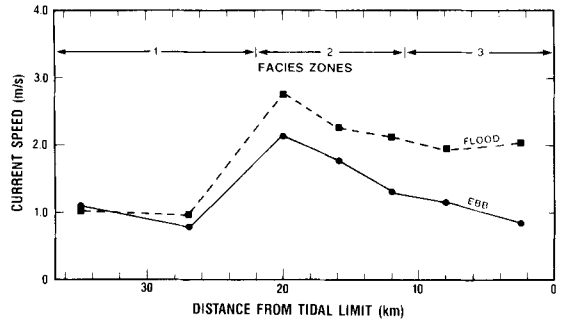

Fig. 5. Longitudinal variation of average-maximum current speeds within the axial sand facies, as measured 1 m above the bed (after Zaitlin, 1987, Fig. 4.9). Values have been averaged over all current meter sites to remove local variations in the degree of ebb and flood dominance.

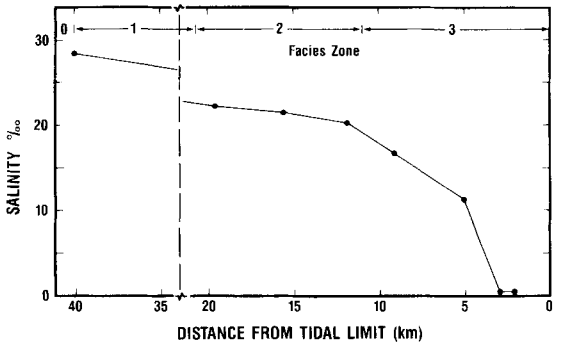

Fig. 6. Longitudinal distribution of salinity at high tide (after Zaitlin, 1987, Fig. 4.2) as measured at average river discharge. The value at 40 km is from Amos & Long (1980).

SSC values reaching nearly 2000 mg l^{-1} have been measured in the turbidity maximum which lies within zone 3 at high tide (Zaitlin, 1987). The available data suggest that the turbidity maximum undergoes an excursion of 25–30 km during every tidal cycle, coming to rest over the subtidal, western portion of the zone 1 sand bars at low tide.

Sediment sources and inputs

The amount of sediment introduced to the Minas Basin–Cobequid Bay system by rivers is estimated to be only $5{\cdot}9 \times 10^4$ m^3 yr^{-1}, with most of this consisting of silt and clay (Amos & Long, 1980). Considerably more silt and clay ($1{\cdot}6 \times 10^6$ m^3 yr^{-1}) is believed to enter the Minas Basin from the main Bay of Fundy, but the largest volume of sediment ($3{\cdot}1 \times 10^6$ m^3 yr^{-1}) is contributed by shoreline erosion. Because the shore cliffs consist primarily of friable Triassic sandstone and unconsolidated Pleistocene outwash, the sediment released is dominated by sand-sized material (7% gravel, 58% sand and 35% silt and clay; Amos & Long, 1980). Much of this sediment is moved eastwards into Cobequid Bay by tidal currents and waves. The above authors estimate that $0{\cdot}85 \times 10^6$ m^3 of bed material (mainly sand) and between 0·3 and $8{\cdot}4 \times 10^6$ m^3 of suspended sediment enters Cobequid Bay each year. A comparison of the 1858 and 1976 bathymetric charts for zone 1 shows that the sand bars have experienced a net accretion of $0{\cdot}7 \times 10^6$ m^3 yr^{-1} (Amos & Long, 1980); presumably the remainder of the sand and most of the mud is accumulating further headward, although there may be some export of mud along the south shore of Cobequid Bay (Amos & Alfoldi, 1979). Amos & Long (1980) estimate that the rate of sediment input has increased by an order of magnitude over the last 7000 years due to tidal amplification. The stratigraphic implication of these data will be discussed following the description of the various facies zones.

SUBTIDAL LAG (ZONE 0) AND INTERTIDAL FORESHORES

Most of the subtidal floor of the Minas Basin and Cobequid Bay seaward of the estuarine sand body (i.e. zone 0) is covered by a 0·1–0·5-m-thick layer of shell-rich gravelly sand, sandy gravel and gravel (Fig. 7; Amos, 1978; Amos & Long, 1980). This coarse material is supplied by ice rafting, and/or represents a winnowed lag of local derivation. The presence of attached organisms indicates that it is immobile (Amos, 1978). In a few areas, such as along the south shore of the Minas Basin and near Economy Point (Figs 2 & 7; Swift & McMullen, 1968; Klein, 1970), localized accumulations of sand overlie this lag, but on the whole, zone 0 is non-depositional.

The foreshores which border the Minas Basin and the zone 1 sand bars in Cobequid Bay (Fig. 8A) average 1–2 km in width, have an average slope of 0·5°, and are backed by cliffs which are eroding at an average rate of 0·55 m yr^{-1} (Amos & Long, 1980). As is the case with zone 0, these wave-cut platforms are generally erosional or non-depositional. In most places, the underlying till or bedrock is mantled by a thin (0·2–0·5-m), sandy gravel lag (Klein, 1963; Dalrymple *et al.*, 1975; Knight & Dalrymple, 1975, 1976) which is continuous with the subtidal lag described above (Fig. 8B) and the sandy gravel beach

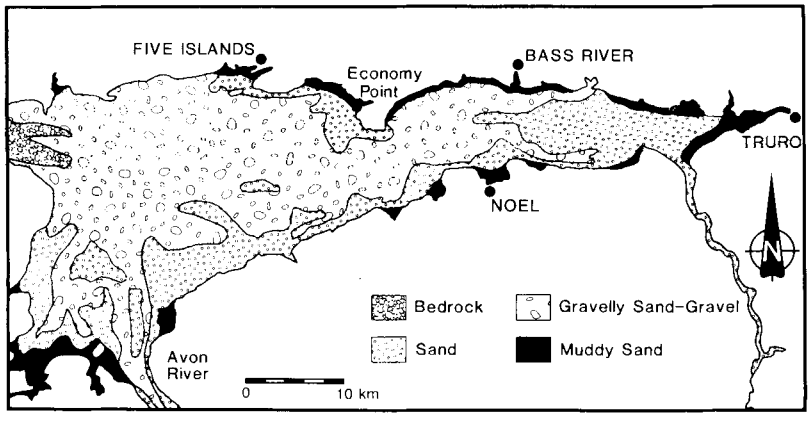

Fig. 7. Distribution of sediment types in the Minas Basin and Cobequid Bay (after Amos & Long, 1980, Fig. 9.11). Details at the head of Cobequid Bay are inexact due to the complexity of the sediment distribution (Fig. 2).

which occupies the interval between the neap and spring high-tide elevations (Fig. 8A, D, E). This lag is exposed over most of the lower foreshore, although it may be covered locally by small amounts of coarse sand (Fig. 8C); on the upper part of the foreshore, it is covered by a thin (0·05–0·5-m) layer of tidal sediment (Fig. 8A, D) which fines landward from sand to silty sands, sandy silts and clayey silts (Klein, 1963; Yeo & Risk, 1981). Because of the relatively high salinity in this part of the system at high tide (Fig. 6), this muddy veneer contains a diverse fauna and is intensely bioturbated (Risk & Yeo, 1980; Yeo & Risk, 1981). These fine-grained sediments occur on the upper foreshore because the tidal-current speeds decrease landwards, and because the exposure time is longer and the resistance to erosion is higher than at lower elevations (Amos & Mosher, 1985). However, the longer-term erosional character of the foreshores, which is due to the confinement by the valley walls (Fig. 3A; see preceeding discussion), suggests that this veneer has a low preservation potential. Indeed, even the thicker accumulations of mudflat and salt marsh sediments which occur in tributary valleys (Fig. 2) are generally fronted by an erosional cliff and a sandy gravel beach (Fig. 8E).

TIDAL SAND-BAR COMPLEX (ZONE 1)

Morphology

The complex of sand bars and channels which constitute facies zone 1 stretches 21 km from Burntcoat Head to Salter Head, and has an average width

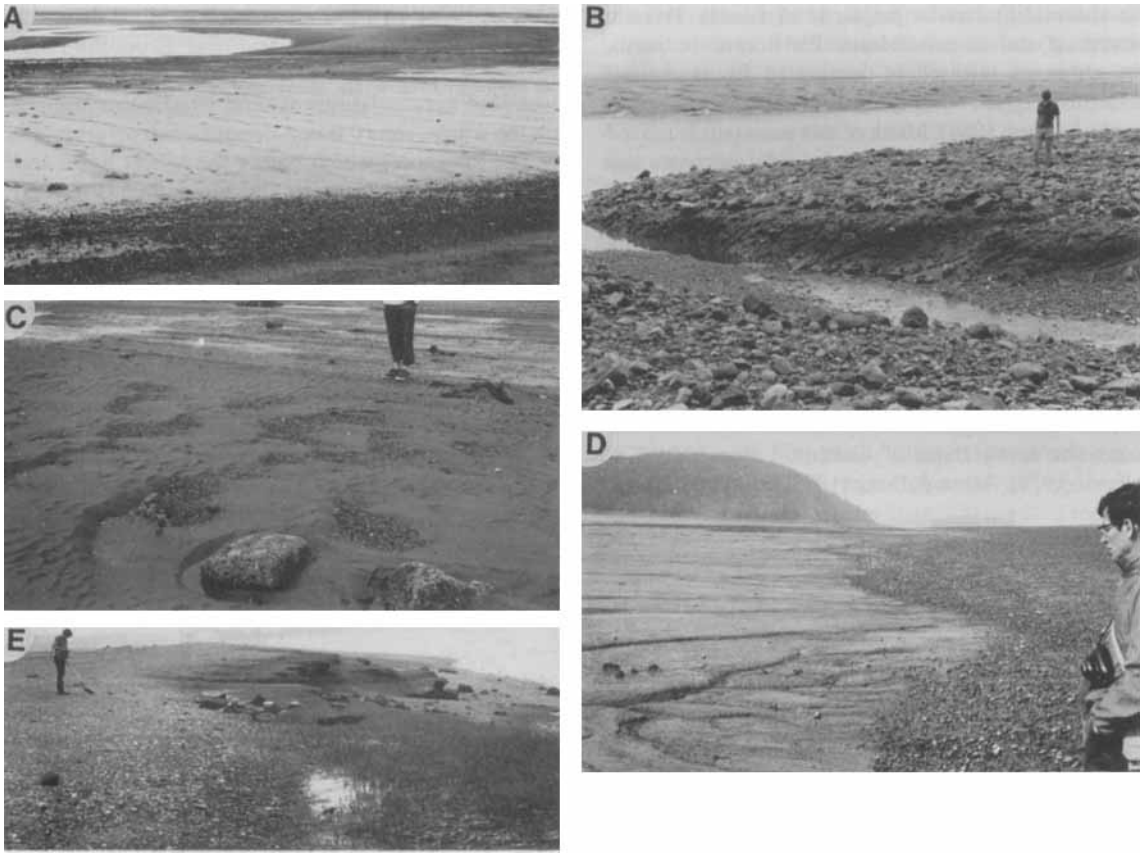

Fig. 8. (A) Facies zonation on the intertidal foreshore adjacent to Selmah Bar (cf. Knight & Dalrymple, 1975): gravel beach (foreground); muddy veneer over lag gravel; exposed gravel lag; and sand bar (background). (B) Lag gravel overlying till on lower foreshore. (C) Starved dunes and ice-rafted boulders with sand shadows (foreground) and current-parallel harrow marks (background) on lower foreshore. (D) Abrupt contact between gravel beach and muddy veneer on upper foreshore. (E) Erosional outer margin of salt marsh overlain by beach gravel, north shore of Cobequid Bay.

of 6–7 km (Fig. 2). These sand bars are underlain by Triassic sediments and a pre-modern unit up to 13 m thick (Fig. 9A, B) which contains Pleistocene till and outwash, and Holocene barrier/lagoonal sediments of the preceeding mesotidal stage (Fig. 4; Knight, 1977, 1980; R. Dalrymple, unpublished data). The thickness of the modern sand body is highly variable, ranging from zero in the deeper channels, to 10–15 m beneath the main bar crests (Fig. 9C). Only locally does the topography of the underlying material control the location of channels or bar crests; consequently, the morphology of the bar complex is determined almost entirely by the modern tidal processes and is constantly changing (see Morphological Evolution below). Because most of the sedimentological data to be presented were collected during the period 1971–1974, the configuration which existed at that time will be described here using the present tense.

The (1971–1974) sand-bar complex contains three major, E–W channels (Figs 2 & 10), the two deepest

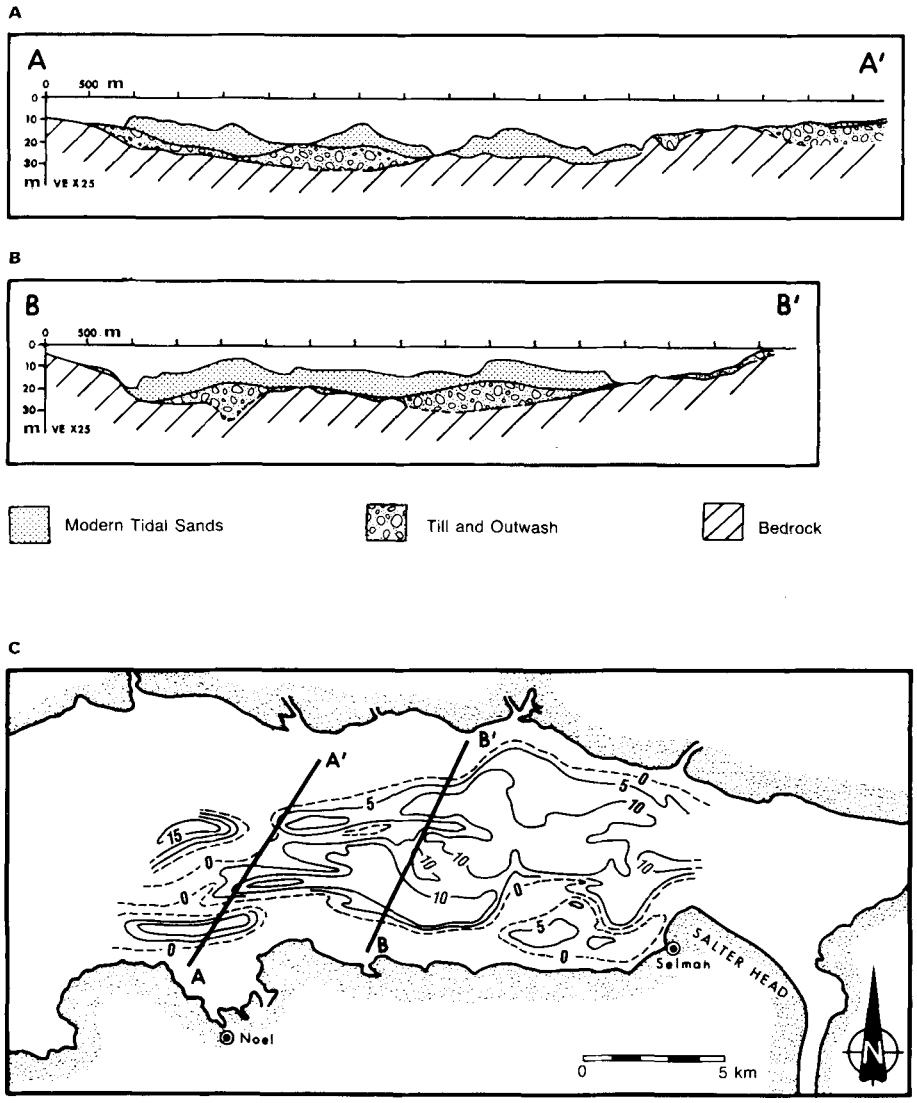

Fig. 9. (A) and (B) Interpreted seismic sections through tidal sand bars (after Knight, 1980, Fig. 10.9, lines 8 and 6 respectively). (C) Isopach map (in metres) of zone 1 sand body, based on 1973 data, showing locations of sections in A and B (after Knight, 1977, Fig. 3.12).

lying along the northern and southern margins of the bar complex, adjacent to the foreshores, whereas the third channel system occupies the centre of the Bay. This latter channel is shallower than the marginal channels, particularly in the outer half of the zone, and portions of its floor are exposed at low tide (Figs 2, 9 & 10). At their western end, the thalwegs of the main channels lie 15 m below lowest low water while the highest bar crests extend 1–2 m into the intertidal zone, producing a relief of over 15 m (Fig. 10). At the east end of the bar complex, the channel bases are approximately 15 m higher, but retain 2–3 m of water at low tide because of the water-surface gradient. Bar-crest elevations also rise eastward, but not as rapidly as the channel bottoms; at Salter Head they extend only 6–7 m above the low-water level, giving a relief of about 10 m (Fig. 10). This headward rise of the bar crests may be a result of several factors including: the eastward rise in the elevation of the underlying substrate (Knight, 1980); and an eastward increase in the extent of sediment infilling (Harris, 1988).

The bars which separate the three channels form two semi-continuous, levee-like, bar chains; the northern chain consists of Great Village Bar, Diamond Bar and the unnamed, subtidal bar south of Bass River, whereas the southern chain consists of Selmah and Noel Shore Bars (Figs 2 & 10). Both of these bar chains attach to the shoreline at their eastern end (i.e. at the heads of Great Village and Selmah Bars), so that the two marginal channels terminate at these locations. By contrast, the central channel is continuous with the channels of the Salmon and Shubenacadie Rivers (Figs 10 & 11). The continuity of both bar chains is broken by a number of diagonal channels termed 'swatchways' (Robinson, 1960), which converge headward on the central channel. The larger swatchways, such as that between Selmah and Noel Shore Bars (relief exceeding 10 m; Figs 2 & 10), are used to delineate individual bars, which reach 5–10 km in length, but numerous smaller swatchways (relief 1–5 m) also occur within Selmah and Great Village Bars at the eastern end of the zone. These smaller swatchways subdivide the bars into 'bar segments' that range in length from a few hundred metres to 2–3 km (Figs 2, 10 & 11–14). Swatchways are not common in the outer half of the complex, and the bars there tend to be narrower and more continuous than those further east (Figs 9C & 10).

On each bar or bar segment, the highest crestal elevation occurs near the eastern end, so that the western side of each swatchway is steeper than the eastern side (Figs 14A & 15A). These steeper flanks have slopes that range from 2–3° in large swatchways (Fig. 12B, C), to the angle of repose in small ones (Fig. 12A). The bar chains also display a N–S asymmetry; the steeper side (4–12°) slopes into the central channel whereas the gentler side (1–5°) dips outward, to the north or south (Figs 9B, 10, 14A & 15A).

Tidal currents and sediment transport patterns

Because of the asymmetry of the tidal wave in Cobequid Bay (flood of shorter duration than the ebb), the maximum flood-current speeds exceed those of the ebb throughout most of the sand-bar complex (Fig. 5). This in turn produces a headward residual transport of sand (i.e. a flood dominance). Extensive observations show, however, that the pattern of residual transport is extremely complex in detail (Figs 13A, 14B & 15B), due to the influence of the bar topography

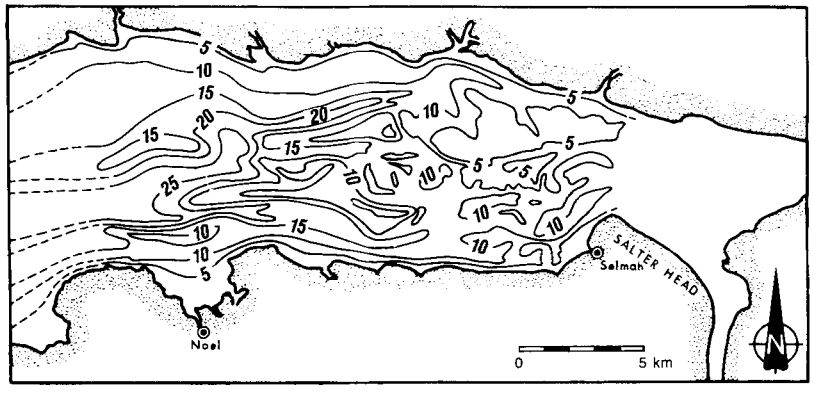

Fig. 10. Bathymetry (in metres) of the zone 1 sand bar complex, based on data collected in 1973 (after Knight, 1980, Fig. 10.5B). Map datum is approximately mean high water.

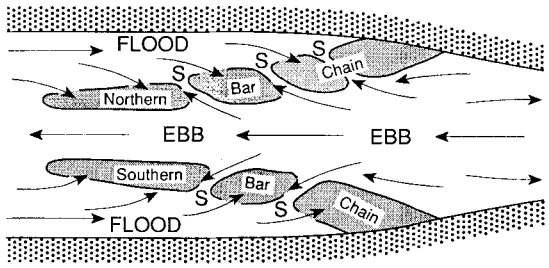

Fig. 11. Schematic illustration of sand bar complex (zone 1) showing morphological elements and net sediment-transport pathways (based on the 1973 morphology). S-swatchway. See text for additional discussion.

and the ebb-tidal discharge from the head of the estuary. The nature of these controls can be illustrated by examining the flow patterns over a tidal cycle (Knight, 1980, Fig. 10.18).

At the start of the ebb, the bar crests are covered by 5–15 m of water so that the topography exerts little influence on the currents and they flow to the west, approximately parallel to the shorelines of the bay. Because the bar chains are slightly oblique to the shorelines (Figs 10 & 11), the flow crosses the bar crests at a low angle (generally $<20°$), passing from the central channel outward into the marginal channels. As it passes over the bar crests, the currents accelerate up the bay-centre flank of the bar and decelerate down the other side, producing enhanced and reduced sediment transport in the two areas respectively. When the bar crests become exposed, the ebb enters a channelized phase in which the flow speeds are strongly influenced by the hypsometry of the up-current areas. The headward-terminating marginal channels are largely isolated from the main ebb discharge from the head of the estuary, and flow speeds may decrease significantly. In the central channel, the opposite generally occurs due to the reduction in the cross-sectional area. Late in the ebb, flow in the central channel is largely independent of the tidal wave, and is controlled instead by the channel slope as in a river.

As the tide starts to flood, ebb flow continues in the central channel because of the seaward-directed hydraulic gradient. Consequently, the incoming tide is diverted around the ebb jet, causing an interdigitation of simultaneously flooding and ebbing currents at the seaward end of zone 1 (Knight, 1980, Fig. 10.17). The zones of flood inflow are confined to the marginal channels, and to two other headward-terminating channels (termed 'flood barbs' by Robinson, 1960), one north of Noel Bay Bar and the other at the west end of Noel Shore Bar (Figs 2 & 13A). Water levels in these regions rise slightly higher than in the adjacent ebb streams. When the bar crests submerge, the resulting transverse pressure gradients cause the flood currents to flow up and over the bar crests, in the opposite direction to that which existed during the ebb, thereby reversing the areas with stronger and weaker sediment transport. As a result, the central channel and its steep flanks have ebb-dominant, westward transport, whereas the marginal channels, flood barbs and gently sloping bar surfaces are generally flood dominated (Fig. 13A). Thus, the bar complex as a whole has the flow patterns and morphology of an ebb-tidal delta (Hayes, 1975), with the bar chains corresponding to the 'channel margin linear bars' (Dalrymple, 1977; Knight, 1977, 1980; Dalrymple *et al.*, 1982; Dalrymple & Zaitlin, 1989). The general pattern of residual transport consists of two sediment-circulation cells, each centred on a bar chain, a northern one with clockwise transport, and a southern one with anticlockwise movement (Fig. 11).

This simple picture is complicated by the swatchways, which form as a result of the between-channel pressure gradients. During the ebb, the swatchways direct a portion of the flow into the marginal channels, subjecting the steep, western side of the swatchway to the full force of the ebb currents while the eastern flank is in the lee of the upstream bar crest (Figs 14B & 15B). On the flood, the current direction and areas of strong and weak flow are reversed. Consequently, the steeper, west side (which is shown below to be an area of active deposition) is ebb-dominated, whereas the east side is flood-dominant (Figs 14B & 15B).

The residual transport patterns (Figs 13A, 14B & 15B) show that all bar crests are maintained by an oblique convergence of sediment. This convergence does not result from helical flow as suggested by Houbolt (1968) and Caston & Stride (1970), but is instead caused by the reversing, cross-ridge component of flow (Dalrymple, 1977; Knight, 1977, 1980; Huthnance, 1982). Conversely, channels are zones of transport divergence; however, unlike bar crests which everywhere have opposing dominances on either side, some channels (including many of the main ones) exhibit the same direction of residual transport across their entire width, whereas others (including the swatchways) have oppositely directed transport on either side of the thalweg (Figs 13A, 14B & 15B). The general asymmetries of the bar chains (steeper toward the central channel) and individual bars and bar segments (steeper to the east) are all

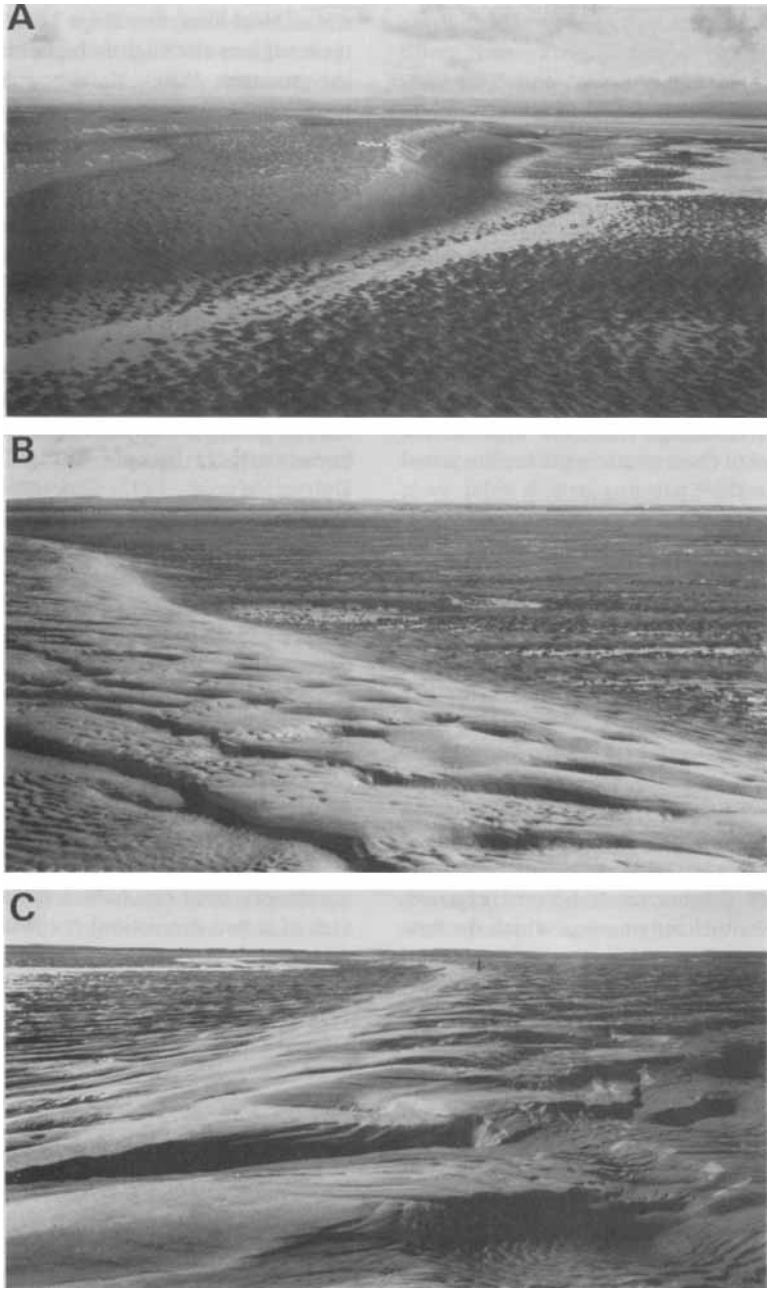

Fig. 12. Depositional western margins of swatchways; see also discussion in Morphological Evolution section. (A) Small swatchway (relief 1·3 m) with superimposed, flood-asymmetric, 2-D megaripples. The structure being produced consists of large-scale, medium-angle cross-bedding (cf. Fig. 20E). (B) Small swatchway (relief 1·2 m) with small, 3-D megaripples. Migration of flood megaripples down this swatchway margin generates inclined cross-bedding like that seen in sandwaves (cf. Fig. 20C, D). Note that ebb flow in the swatchway thalweg is parallel to the channel margin. (C) Large swatchway (relief nearly 4 m); figure in centre distance for scale. Ebb flow is approximately parallel to the strike of the slope. In (B) and (C), wave activity during emergence has partially destroyed the bedforms on the steeper slopes.

consistent with the general dominance of the flood-tidal currents (Figs 5 & 13A).

Although the *relative* strengths of the flood and ebb currents determine the dominant transport directions and, thus, the bar morphology, it is the *absolute* value of the average-maximum current speed during the dominant tide which determines the grain size, bedform type and sedimentary structure present at most locations (Dalrymple *et al.*, 1978; Dalrymple, 1984a). The areal distribution of the average-maximum speeds (Figs 13B, 14B & 15B) shows that they correlate strongly with water depth; without exception, the highest speeds occur in the swatchways and major channels, where values are generally greater than 1·25 ms^{-1} and locally exceed 2 ms^{-1}. In the marginal flood channels, speeds decrease headward due to the decreasing tidal prism, reaching maximum values of less than 1 ms^{-1} where the bar chains attach to the foreshore (Figs 13B & 14B). In the main ebb channel, by contrast, the speeds of the dominant, ebb currents decrease seaward through zones 1 and 2 (Fig. 13B), because of the loss of discharge through the swatchways and/or a decrease in the water-surface slope. Throughout zone 1, bar crests have much lower current speeds (commonly <1 ms^{-1}) than the channels because of the shallow water depths and greater relative friction. The areal extent of these low speeds increases headwards as the bars rise in elevation (Figs 13B, 14B & 15B); as a result, the spatial variability of current speeds is greatest at the east end of the bar complex.

Sediment grain sizes

The distribution of mean grain sizes (Figs 13C, 14C & 15C) shows that several clearly defined trends occur throughout the sand-bar complex. In the marginal flood channels, the sediments fine headward, from very coarse sand and gravel (mean sizes <0 phi) at the seaward end, to medium sand (1–2 phi) at their eastern end. The sand in the ebb channel also fines headward, from medium and coarse sand at the west end to fine sand in zone 2 (Figs 13C, 14C & 15C). However, these sediments are generally finer than those in the adjacent flood channels (Figs 14C & 15C), and lack the coarse traction population (Middleton, 1976) which is a prominent feature of the flood-dominated areas (Fig 16, cf. samples A–D with E). The bar crests, which are finer grained than either of the adjacent channels, also fine eastward, from medium sand on Noel Bay Bar and the eastern end of Noel Shore Bar, to fine and very fine sand at the head of the bar chains (e.g. Selmah Bar; Fig. 14C). The swatchways disrupt these trends, however, by allowing coarser sand to be transported toward the Bay centre on the flood-dominated, eastern flank of each swatchway, while finer sand is carried toward the marginal channels along the ebb-dominated, western side (Figs 14C & 15C). The effect of these conflicting tendencies is dependent on the extent to which each swatchway is flood or ebb dominated: if the swatchway is strongly flood dominated, its (depositional) western flank will fine upwards (Figs 14C & 17A, B, E), whereas this side will coarsen upwards (Figs 15C & 17C, D) if the swatchway is more strongly ebb dominated.

The eastward- and crestward-fining trends which exist in the flood-dominant parts of zone 1 (Figs 13C, 14C & 15C) occur because the flood-current speeds decrease in these directions (Figs 13B, 14B & 15B). As the relatively coarse sediment which enters these areas from the west is carried into regions with lower current speeds, the traction and intermittent suspension populations progressively shift to finer sizes due to selective deposition of their coarse tail (Fig. 16, samples A–D; Middleton, 1976). As a result, the grain sizes within the flood-dominated areas are generally in equilibrium with the prevailing average-maximum flood currents (Dalrymple, 1977). This is not the case in the ebb-dominant areas, however, as grain sizes are finer than the predicted competence of the currents. This situation also exists in zones 2 and 3 where fine to very fine sand (Figs 13C & 16) occurs in areas with speeds in excess of 2 ms^{-1} (Figs 5 & 13B).

It is thought that the disequilibrium in these areas results from a large-scale hydraulic sorting process (Fig. 13D) similar to that proposed for the Avon River estuary (Fig. 1C; Lambiase, 1977, 1980a; Dalrymple & Zaitlin, 1989). Because most of the material entering the estuary does so from the seaward end, it must pass through the flood-dominant portions of zone 1 before reaching the central ebb channel or zones 2 and 3. As it moves eastward, the low current speeds on the bar crests cause the coarser fractions to be deposited; consequently, only a limited amount of the traction population leaks into the central channel by way of the swatchways (Figs 13C & 14C), and the central channel becomes finer grained than the flood channels (Fig. 13C). Furthermore, because both of the major flood channels terminate at the headward end of zone 1, sediment *must* pass through the ebb-dominated zone north of Salter head (Fig. 13A) in order to reach zone 2. Because particles comprising the traction population are moved a very short distance during each tide (Dalrymple, 1977, 1980), any of this material

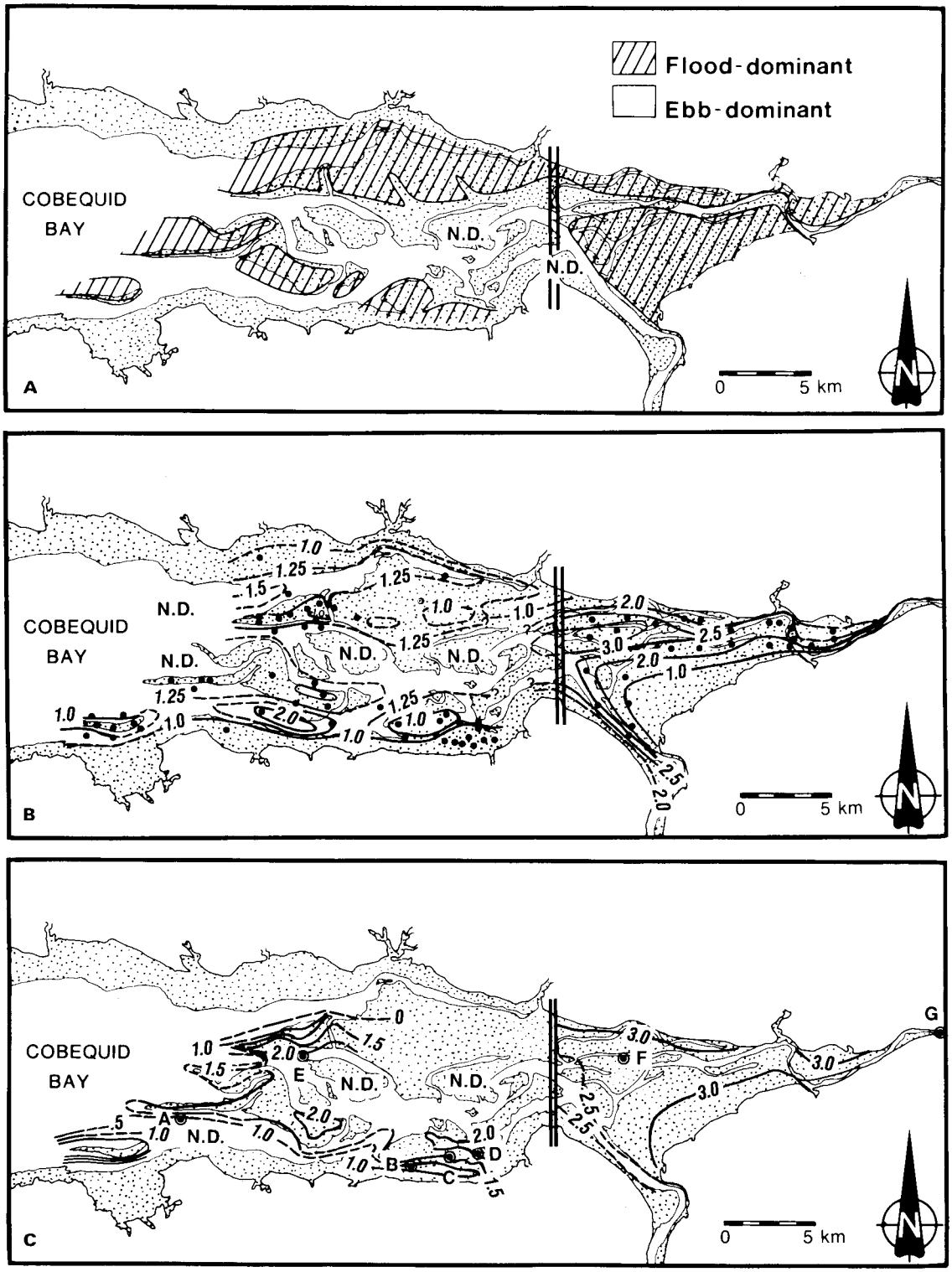
Flood-dominant
Ebb-dominant
COBEQUID
BAY
N.D.
N.D.
A
0
5 km
N
COBEQUID
BAY
N.D.
N.D.
N.D.
N.D.
N.D.
1.0
1.25
1.5
2.0
2.5
3.0
B
0
5 km
N
COBEQUID
BAY
N.D.
N.D.
N.D.
A
B
C
D
E
F
G
0
1.0
1.5
2.0
2.5
3.0
C
0
5 km
N

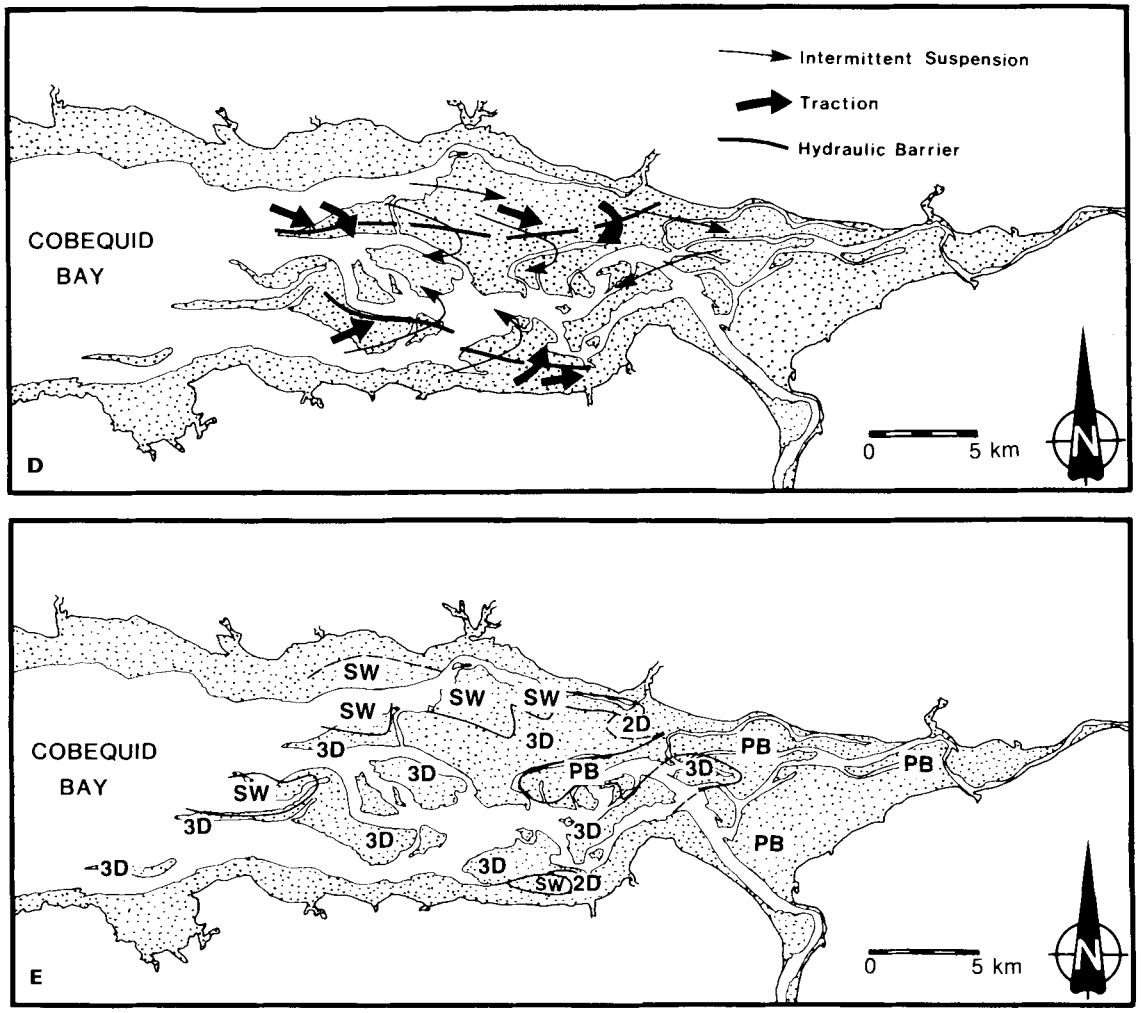

Fig. 13. Sedimentary dynamics of the Cobequid Bay–Salmon River estuary. Throughout, the morphological outline and sedimentological data for zone 1 were obtained in 1971–1974 (Dalrymple, 1977; Knight, 1977), whereas the data for zones 2 and 3 were collected in 1984–1985 (Zaitlin, 1987). (A) Distribution of ebb- and flood-dominant areas. ND–no data. (B) Average-maximum speeds (in ms^{-1}) of the *dominant* tidal current. Data for zone 1 are depth-averaged values, whereas values for zones 2 and 3 were recorded 1 m above the bed. (C) Mean grain size in phi units. Dots and letters refer to samples shown in Fig. 16. (D) Schematic illustration of the hydraulic sorting process responsible for the exclusion of medium and coarse sand (traction population) from zone 2. (E) Distribution of bedform types: 2D–2-D megaripples, 3D–3-D megaripples, SW–sandwaves, and PB–upper-flow-regime plane bed.

which reaches this ebb-dominated area will be unable to pass through it, and will be carried back seaward (Lambiase, 1980a). Intermittently suspended particles may, however, hop over this ebb barrier, because of the greater distances moved in a single flood tide. As a result, the sands of zones 2 and 3 generally contain only an intermittent-suspension population (Fig. 16, samples F & G; Maher, 1986; Zaitlin, 1987).

Bedforms and sedimentary structures

Because the average-maximum current speeds of the dominant tide are almost nowhere less than $0{\cdot}8\ ms^{-1}$ in zone 1 (Fig. 13B), ripples and 2-D megaripples (Fig. 18A), which form at these low speeds (Dalrymple *et al.*, 1978), are not as widespread as the dominant (i.e. largest) bedform type. These bedforms occur by themselves only in limited areas on bar crests,

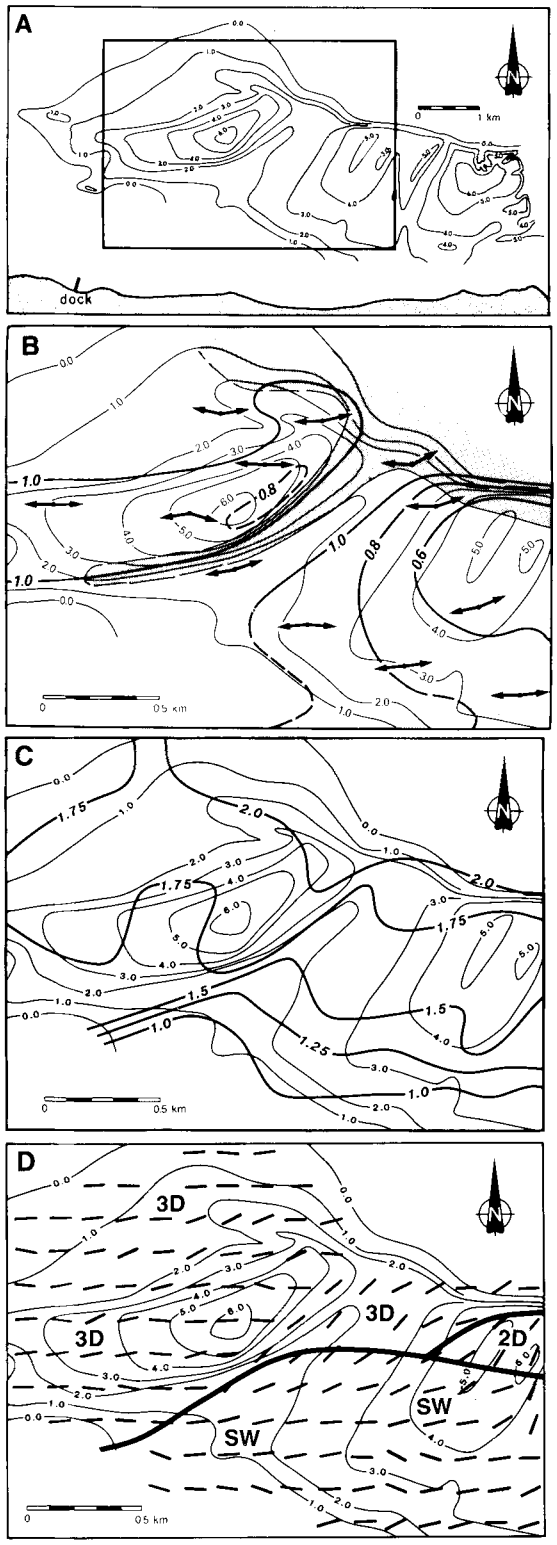

particularly at the eastern end of the bar chains (Figs 13E & 14D). Instead, 3-D megaripples (Fig. 18B) and sandwaves with superimposed megaripples (Fig. 18C, D; Dalrymple, 1984a) are the dominant bed configurations throughout most of the bar complex. For reasons which are unknown, sandwaves are restricted to sediments with mean sizes coarser than approximately 0·31 mm (1·7 phi; Figs 13C, E & 14C, D; Dalrymple *et al.*, 1978); therefore, they occur almost exclusively in the flood-dominant portions of Cobequid Bay (Figs 13E, 14D & 18D). The finer-grained, ebb-dominant channel, by contrast, contains only 3-D megaripples (Figs 13E & 18B), except at its eastern end where grain sizes drop below 0·175 mm (2·5 phi) and upper-flow-regime plane bed occurs (Figs 13E & 28A). Similar grain-size controls exist on the distribution of bedform types in the individual swatchways (Fig. 14C, D). In general, bedform height tends to decrease as the water depth and maximum current speed decrease, so that the smallest bedforms tend to occur on bar crests (Fig. 19). It is important to note that no sharp distinction in either bedform height or type occurs at the low-water level.

Megaripple orientations generally correspond to the predominant E–W flow direction of the peak tidal currents; thus, most bedform migration is at a small angle to the bar crestlines (Fig. 14D). Sandwaves are, however, commonly skewed relative to the dominant currents (by 24° on average) because of variations in migration speed along their length (Dalrymple, 1984a); the sandwaves and superimposed megaripples thus commonly show divergent orientations (Fig. 18C, D). Deviations from the general E–W pattern of bedform migration are greatest (up to 80°) in the thalweg and along the western flank of swatchways, where the flow is deflected into a swatchway-parallel orientation (Figs 12B, C & 14D).

Fig. 14. Distribution of hydraulic and sediment characteristics in the large swatchway on Selmah Bar (Figs 2 & 27). All data are from Dalrymple (1977) and Knight (1977). (A) Topographic map (in metres) of Selmah Bar as surveyed in 1971 (after Dalrymple, 1977, Fig. 2.12). Datum is approximately mean low water. The rectangle shows the detailed area shown in (B), (C) and (D). (B) Distribution of the average-maximum depth-averaged speed (in ms^{-1}) of the *dominant* current (heavy contours). The shaded area is ebb dominant. Arrows give flow directions of maximum, ebb and flood currents as measured 1 m above the bed. (C) Distribution of mean grain size (heavy contours) in phi units (after Dalrymple, 1977, Fig. 5.11A). (D) Distribution of bedform types; abbreviations as in Fig. 13E. Short bars are normals to bedform crestlines and indicate general flow directions.

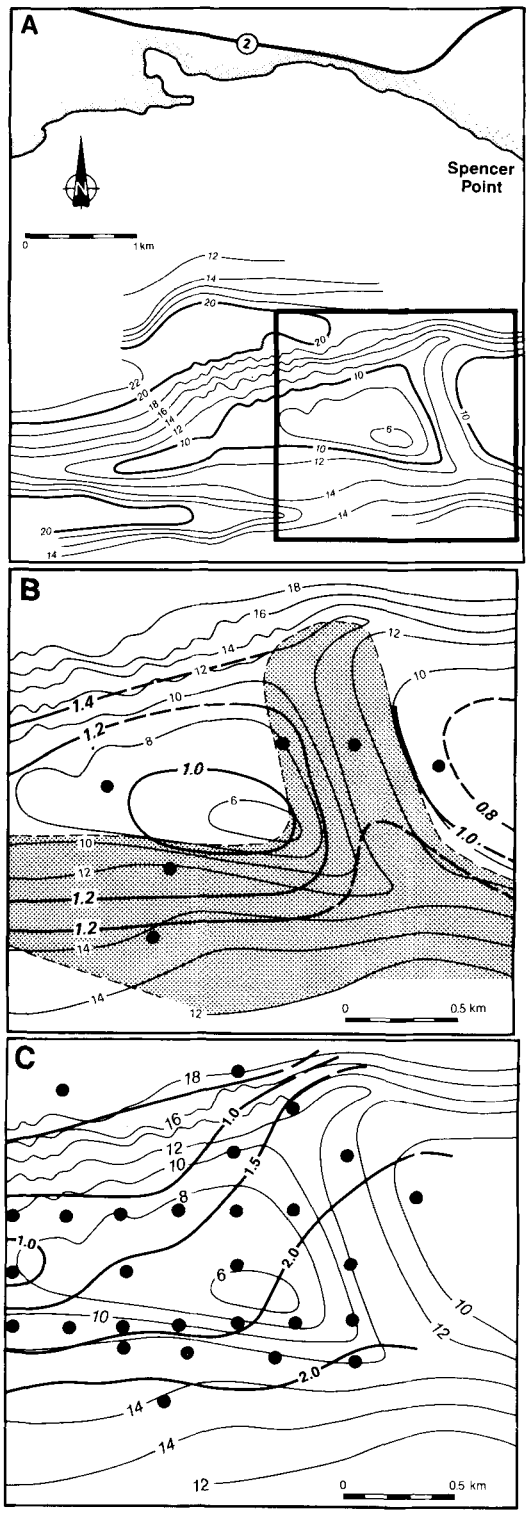

The structures within the sand bars consist predominantly of cross-bedding, but the type varies from place to place because of differences in the type of bedform present (Dalrymple *et al.*, 1978; Harms, Southard & Walker, 1982; Dalrymple, 1984a). The deposits of the ebb channel consist primarily of trough cross-bedding generated by the 3-D megaripples (Fig. 20A, B). Ebb-orientated sets are most abundant, but some flood sets are also present (Fig. 20A). In the base of this channel, upper-flow-regime conditions exist locally at low tide, but the presence of megaripples in many of these areas during the rest of the tidal cycle will probably destroy any upper-flow-regime structures. In the headward parts of the flood-dominated channels and on some bar crests where the current speeds are lowest (Fig. 13A, E), 2-D megaripples produce headward-dipping, planar-tabular cross-bedding. Elsewhere in the flood channels, sandwaves produce more complex cross-stratification (Dalrymple, 1984a). The most common type is inclined cross-bedding in which decimetre-scale cross-beds are themselves inclined in the direction of sandwave migration (i.e. headward) at angles averaging 10° (Fig. 20C, D). Flood-directed sets predominate within such cosets, but ebb-orientated sets are moderately abundant. Inclined sets of parallel bedding may also be present, particularly near the bases of intertidal sandwaves where it is formed either by dewatering outflow (Fig. 23C) or wave action during emergence. In situations where the superimposed megaripples are small relative to the height of the sandwave (e.g. in coarse sand or near the lower current-speed limit of sandwave occurrence), the sandwaves produce simple sets of large-scale, medium- to high-angle cross-bedding (Fig. 20E, F; Dalrymple, 1984a) which grades into the planar-tabular cross-bedding of 2-D megaripples as the superimposed megaripples become smaller. Either the inclined or simple cross-bedding may be overlain by a coset of more-or-less horizontally disposed, interbedded, ebb and flood cross-beds (Fig. 20F; the 'complex coset' of Dalrymple, 1984a) which

Fig. 15. Distribution of hydraulic and sediment characteristics in the swatchway at the east end of Diamond Bar. (A) Topographic map (in metres) of Diamond Bar (Fig. 2; after Dalrymple, 1977, Fig. 2.15). Datum is approximately mean high water. Box indicates area shown in (B) and (C). (B) Distribution of average-maximum, depth-averaged speed (in ms^{-1}) of the *dominant* current (heavy contours; after Dalrymple, 1977, Fig. 3.15B). The shaded area is ebb dominant. Dots indicate current meter stations. (C) Distribution of mean grain size (heavy contours) in phi units (after Dalrymple, 1977, Fig. 5.9A). Dots are sample locations.

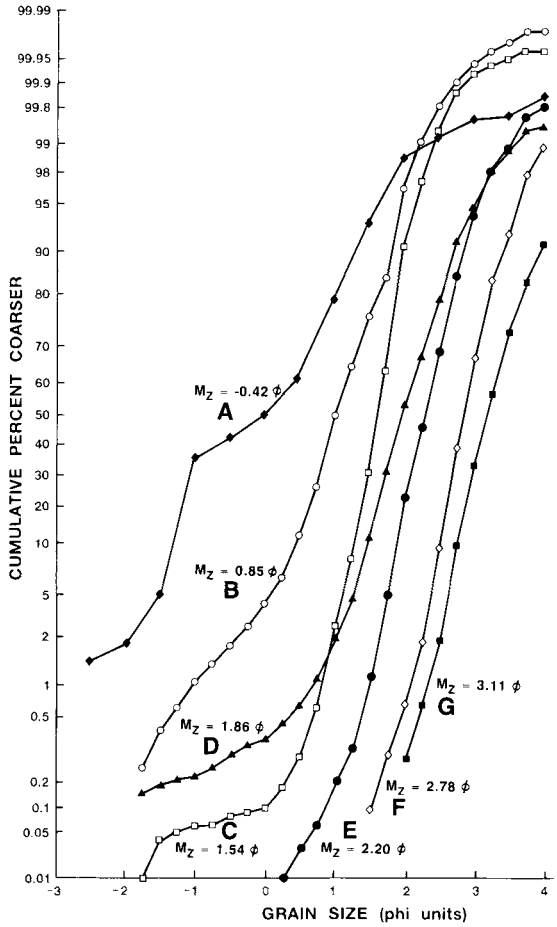

Fig. 16. Typical grain size distributions; see Fig. 13C for sample locations. Data sources: (A) Knight (1977); (B)–(E) Dalrymple (1977); (F) and (G) Maher (1986). M_z–moment mean size. See text for discussion.

are deposited during upward growth of the sandwave crest. It must be emphasized that, because bedform types do not differ between adjacent subtidal and intertidal areas, the major structures will not be significantly different. Minor features are all that distinguish between these two zones.

The subordinate currents cause the bedforms to be reorientated to varying degrees (Figs 18A, D & 21), with the amount of reworking inversely proportional to the size of the bedform and directly proportional to the strength of the subordinate current. The reactivation surfaces produced are not, however, equally abundant in all parts of the complex. In the ebb channels where grain sizes are fine and current speeds high, the 3-D megaripples commonly have net migration distances over one tidal cycle that are a large fraction of, or may even exceed, the bedform wavelength; therefore, reactivation surfaces are widely spaced. By contrast, the 2-D megaripples which occur in some flood-dominated areas have much slower migration rates due to the lower current speeds, and reactivation surfaces are more closely spaced (Fig. 21B). Reactivation surfaces are not common in the sandwave deposits (Fig. 20C–F) because the passage of each megaripple trough over the sandwave brink usually removes the minor erosion surfaces created by the subordinate currents (Dalrymple, 1984a).

Well-developed mud drapes, which are abundant in some tidal settings (e.g. Terwindt, 1981; Allen, 1982), are not widespread here. At high tide, the turbidity maximum lies in zone 3 (Amos & Long, 1980; Zaitlin, 1987), and mud deposition is probably minimal on the sand bars. Mud drapes are more likely to form on the falling tide as the turbidity maximum is advected over the bars, but the slack-water period just prior to the emergence of intertidal areas is only a few minutes long and mud deposition is generally minimal; as a result, mud-impregnation of the surficial sand is much more extensive than discrete mud layers. The longest quiet-water periods occur near the heads of the flood channels; in these areas, mud drapes may be deposited in megaripple troughs (Fig. 22A), especially on calm days, and mud pebbles derived from such drapes are moderately common (Fig. 22B). The subtidal, western part of the bar complex may have an even greater number of mud drapes because the turbidity maximum comes to rest here at low water.

Many other minor features are also created during or after emergence of the intertidal parts of the bars. A spectacular array of late-ebb current ripples is present on most of the larger bedforms at low tide (Figs 18, 20 & 23A). These ripples have orientations which may deviate markedly from those of the dunes (Klein, 1970) because the ripples are commonly produced by flow down the local slope. Runoff microdeltas (Dalrymple, 1984b) are also generated by these flows, which may be sufficiently intense that the primary bedforms are strongly modified or even destroyed (Fig. 23B). The seepage of water from the lee faces of sandwaves can create prominent rill networks and deposit a 'dewatering ramp' at the toe of the slope (Fig. 23C). Wave action may form water-level marks on the lee faces of bedforms (Fig. 23D); wave ripples and combined wave-current ripples are also occasionally abundant. If wave action is intense, however, it will smooth (Figs 12A, B & 24) or even

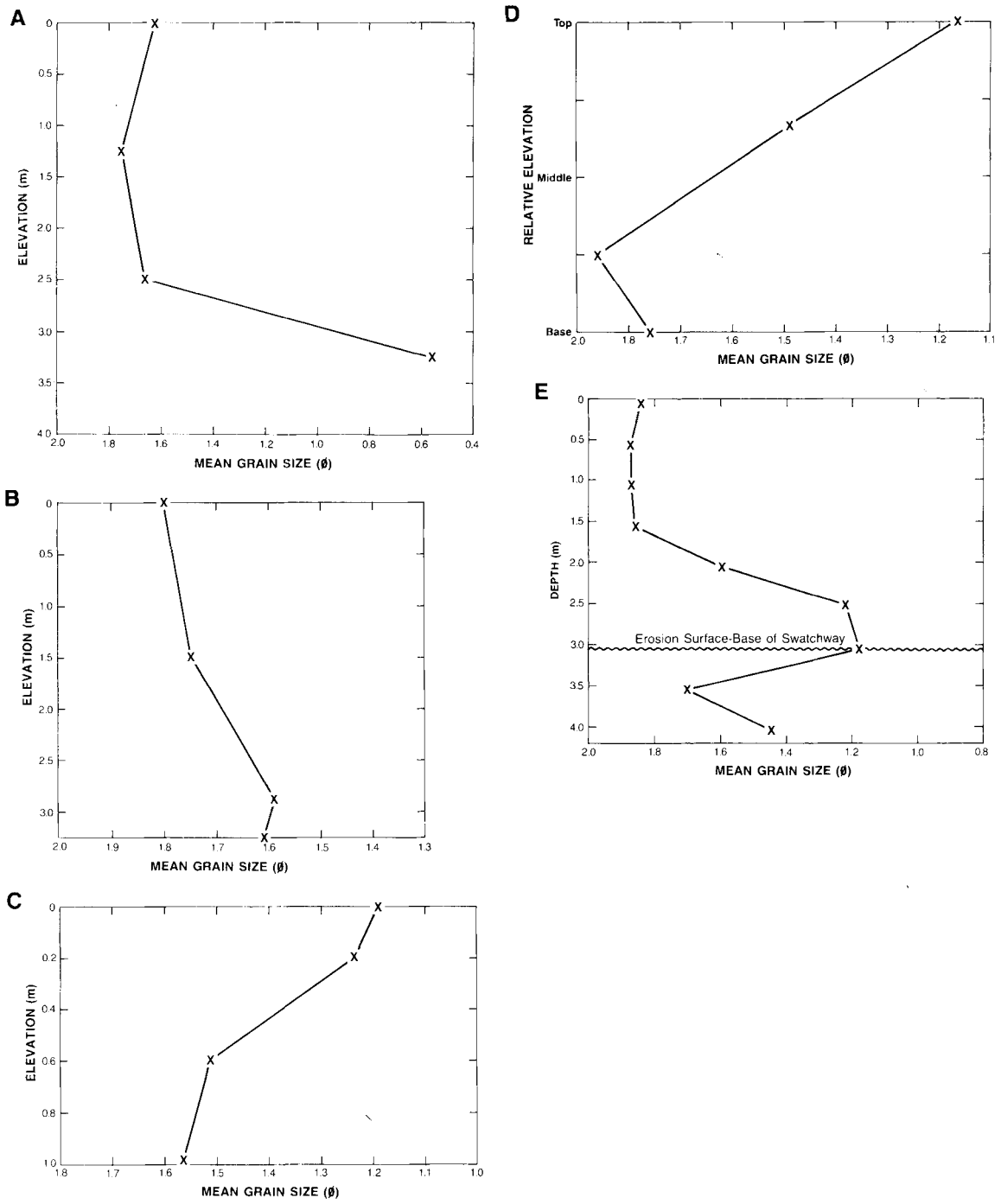

Fig. 17. Variation of mean grain size with elevation on the depositional, western flank of swatchways. From: (A)–(C) Selmah Bar; (D) and (E) Great Village Bar (Fig. 2). (A)–(D) are based on surface samples, and (E) is from a vibrocore adjacent to the depositional flank.

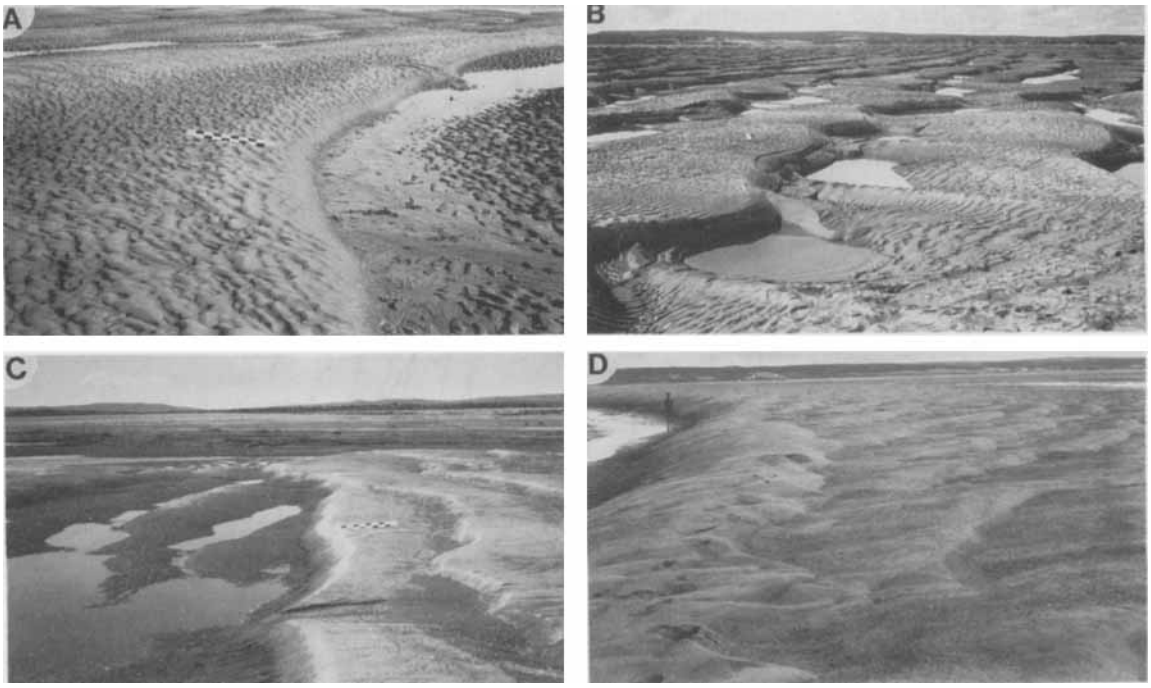

Fig. 18. (A) Flood-asymmetric, 2-D megaripple (medium, 2-D simple dune in the revised terminology of Ashley *et al.*, 1990) covered by ebb current ripples. Metre stick for scale. (B) Ebb-asymmetric, 3-D megaripple (medium, 3-D simple dune; Ashley *et al.*, 1990) with prominent spurs and scour pits. Note the relatively straight crestlines despite the scour pits. (C) Crest (right side of photo) and lee face of ebb-asymmetric sandwave (=large, 2-D compound dune; Ashley *et al.*, 1990) with superimposed megaripples. Note the divergent orientations of the sandwave and megaripples. (D) Flood-asymmetric sandwave (large, 2-D compound dune; Ashley *et al.*, 1990) with superimposed ebb megaripples. Compare profile of this lee face with that in (C), and note the ebb cap in left foreground.

obliterate dunes in exposed areas; flat-topped ripples (Fig. 23E) are a small-scale example of this. Wave action also produces small-scale, soft-sediment deformation structures in megaripples composed of fine sand (Dalrymple, 1979). Wind action is generally not important, but adhesion structures (Fig. 23F) and wind ripples may be formed on occasion. Bubbled sand is generated locally by the rapidly rising flood tide.

Despite the impressive amount of ice which occurs during the winter, structures produced by it are insignificant on the sand bars (Knight & Dalrymple, 1976; Zaitlin, 1987). The only clear evidence of ice action is the presence of out-sized blocks of salt-marsh sediment (Fig. 24) and/or patches of siliciclastic gravel derived from the foreshores.

Biogenic structures are not abundant in the sand bars due to the rapid migration of the large bedforms (Amos *et al.*, 1980; Yeo & Risk, 1981). However, a limited range of organisms does inhabit areas near the heads of the two bar chains where ripples and slowly migrating 2-D megaripples are developed (Fig. 13E). The polychaetes *Spiophanes wigleyi*, *Clymenella torquata* and *Scolecolepides viridis* all produce lined, vertical burrows up to 50 mm long (Fig. 25A; Featherstone & Risk, 1977) which may be preserved, whereas *Polydora* sp. creates an unlined vertical burrow. Another polychaete, *Paraonis fulgens*, makes a lined, horizontal spiral or circular-looped burrow up to 30–40 mm in total diameter (Fig. 25B) at a depth of 50–80 mm in the sand (Risk & Tunnicliffe, 1978). All of these organisms have patchy distributions but occur in large numbers where present.

Morphological evolution

The preceding sections have presented a detailed synthesis of the sedimentary characteristics of the sand-bar complex, based on the data collected in 1971–1974 (Figs 2 & 13). Before these various elements

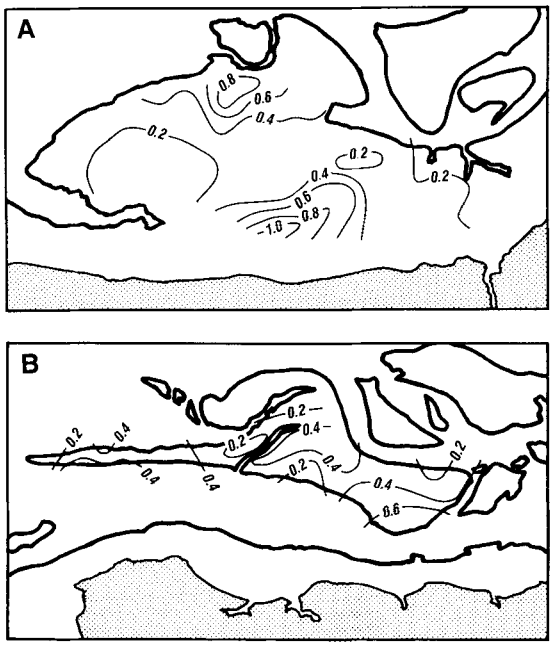

Fig. 19. Distribution of bedform heights (in metres) on (A) Selmah Bar and (B) Noel Shore Bar (Fig. 2; after Knight, 1977, Figs 5.10A & 5.8A respectively). Only the height of the largest bedform type present at any location has been recorded; in areas with sandwaves (cf. Figs 13E & 14D) smaller megaripples are also present. Land is stippled.

can be assembled into a facies model, it is necessary to examine the morphological evolution of the complex over a longer period, in order to determine the larger-scale architecture of the deposits. Historical information from before 1938 is scanty, but since then, periodic, aerial photographic coverage permits documentation of the major morphological changes (Fig. 26).

Despite numerous small-scale changes in the bar outlines, the general organization of the bar chains and major channels appears to have remained the same from 1860 until 1947 (Fig. 26A–C). Through this period, the main ebb channel passed to the north of Salter Head, then gradually curved to the south past the western end of Selmah Bar, and continued westward along the south shore of the bay. As a result of this ebb-channel configuration, the northern bar chain, although dissected by several swatchways and flood barbs (Fig. 26A–C), was longer than it was in 1973 (Fig. 26E), whereas the southern bar chain was much shorter and consisted only of Selmah Bar.

After this long period of relative stability, a major reorganization of the sand-body geometry took place between 1947 and 1961–63 (Fig. 26C, D), such that the ebb channel adopted a straighter course down the centre of the bay, before bifurcating around a diamond-shaped bar (called 'Betsy Bob' Bar by Swift & McMullen, 1968). Apparently, the enlargement of the swatchways in the northern chain between 1938 and the early 1960s (Fig. 26B–D) allowed them to capture a progressively greater share of the ebb flow, until they took over the function of the ebb channel. This new channel configuration persisted in 1973 (Fig. 26E), but the swatchway at the west end of Selmah Bar had grown larger than it was in 1961–63, perhaps because the swatchway that existed to the west of it in 1947 (Fig. 26D) had closed. This trend continued through the 1970s so that by 1982 (Fig. 26F) this swatchway had captured the ebb channel, which had returned to the south-shore position that it had occupied from 1860 to 1947 (Fig. 26A–C). The northern bar chain was again more-or-less continuous from the western end of the sand-bar complex to its shoreline-attachment point north of Salter Head.

It would appear, therefore, that the usual configuration of the Cobequid Bay sand bars consists of a single, predominant bar chain extending diagonally NE–SW across the bay, flanked to the southeast by the ebb channel (Fig. 26A–C, E, F). The larger-scale patterns of tidal flow in the Minas Basin and Cobequid Bay may be responsible for this organization, as observations of the distribution of suspended sediment (Amos & Alfoldi, 1979) and numerical modelling of tidal-current residuals (Greenberg, 1979) indicate that the flood flow into Cobequid Bay is concentrated along the north coast, whereas the ebb flow is strongest on the south shore. Recently collected seismic data (R. Dalrymple, unpublished data) also suggest that a thick body of Pleistocene till and outwash is present beneath Great Village Bar; this may prevent the ebb channel from adopting a more northerly course.

The above illustrates the significance of swatchway growth and closure with regard to the evolution of the large-scale, channel-bar morphology. Detailed observations also indicate that all of the swatchways, regardless of size, migrate to the east because of the flood-current dominance discussed above. On Selmah Bar, measurements using fixed stakes show that the smaller swatchways (e.g. Fig. 12A) migrate eastwards at a rate of approximately 0·25 m per tidal cycle (175 m yr^{-1}). Larger swatchways migrate at correspondingly slower rates; for example, the 5-m-deep swatchway through Selmah Bar (Figs 14 & 27) has migrated a total distance of 2·1 km (61 m yr^{-1}) between 1947 and 1982 (Fig. 27B–E), with the rate

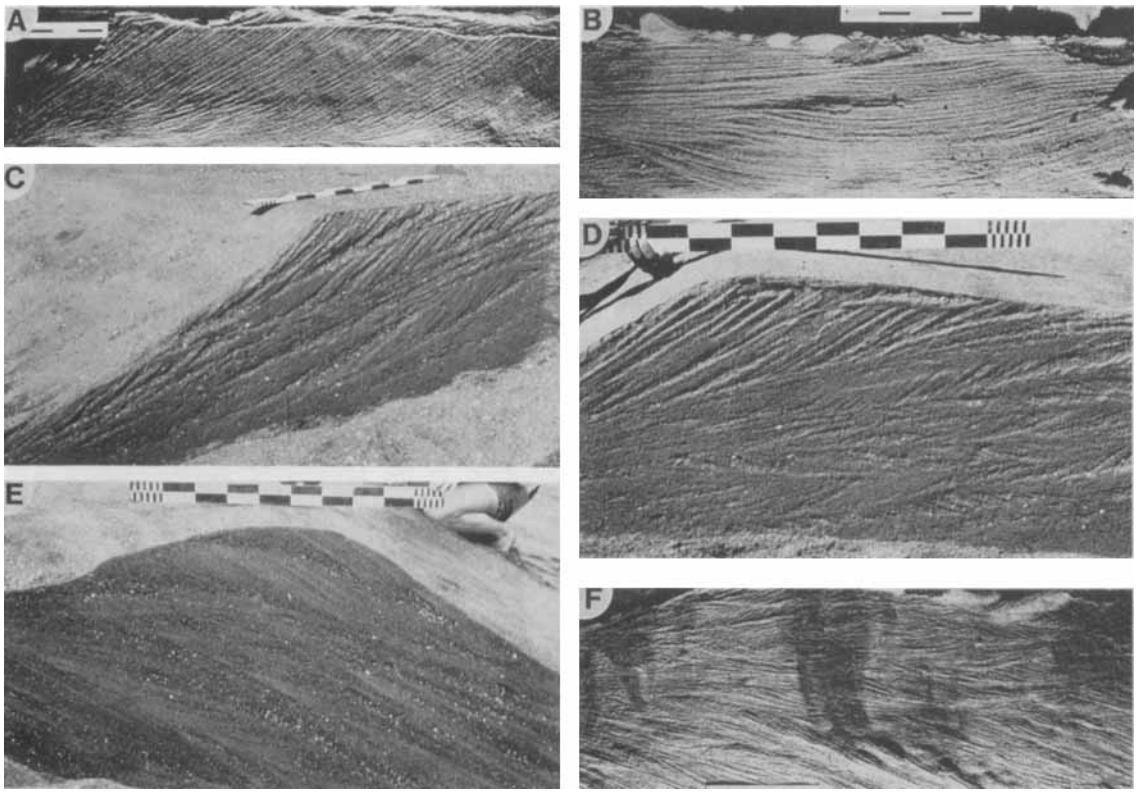

Fig. 20. (A) Epoxy relief peel perpendicular to crestline of a 3-D ebb megaripple. Ebb ripples occur at top of peel, and some flood cross-bedding is present at the base. Note lack of reactivation surfaces. On all peels, scale divisions are 50 mm long. (B) Peel taken parallel to crest of 3-D megaripple showing trough geometry of sets. (C) and (D) Inclined (or compound) cross-bedding within sandwaves; Dalrymple (1984a, Fig. 7A, B). (E) Large-scale cross-bedding within a sandwave; Dalrymple (1984a, Fig. 8A). (F) Peel of a complex coset (Dalrymple, 1984a) overlying large-scale foresets in a sandwave.

increasing from 33 m yr^{-1} (1947–1961) to 76 m yr^{-1} (1961–1973) and then to 82 m yr^{-1} (1973–1982). Since 1961, this eastward migration has also been accompanied by an eastward shift of the facies at the east end of the bar (Fig. 27D, E). A similar headward migration is shown by the swatchways in the central portion of the northern bar chain between 1938 and 1947 (Fig. 26B, C).

Another style of channel behaviour involving a small side branch of the central ebb channel can also be seen in Fig. 27. In 1938 (Fig. 27A) the east end of Selmah Bar was very wide and the northern margin of the bar was essentially straight with an ENE–WSW orientation. By 1947 (Fig. 27B), a small side branch of the ebb channel had cut southward into the east end of the bar, a process which continued, but at a slower rate, until 1982 (Fig. 27C–E). Throughout 1963–1982, there was some filling of this channel, as indicated by the emergence of low bars in its base and the growth of a delta-like sand body at the northern end of the major swatchway (Fig. 27D, E). Observations in 1989 have shown that this channel has now been filled entirely, and the bar outline has returned approximately to its 1938 shape (Fig. 27A).

INNER COBEQUID BAY–SALMON RIVER ESTUARY (ZONES 2 AND 3)

Although the primary focus of this paper is the elongate tidal sand bars of zone 1 (Fig. 2), it is necessary to describe briefly the inner portion of the complex (zones 2 and 3; Fig. 2) before developing a vertical facies model for the entire estuary.

The area between Salter and Lyons Heads (zone 2; Fig. 2) contains a broad, axial sand area that is criss-

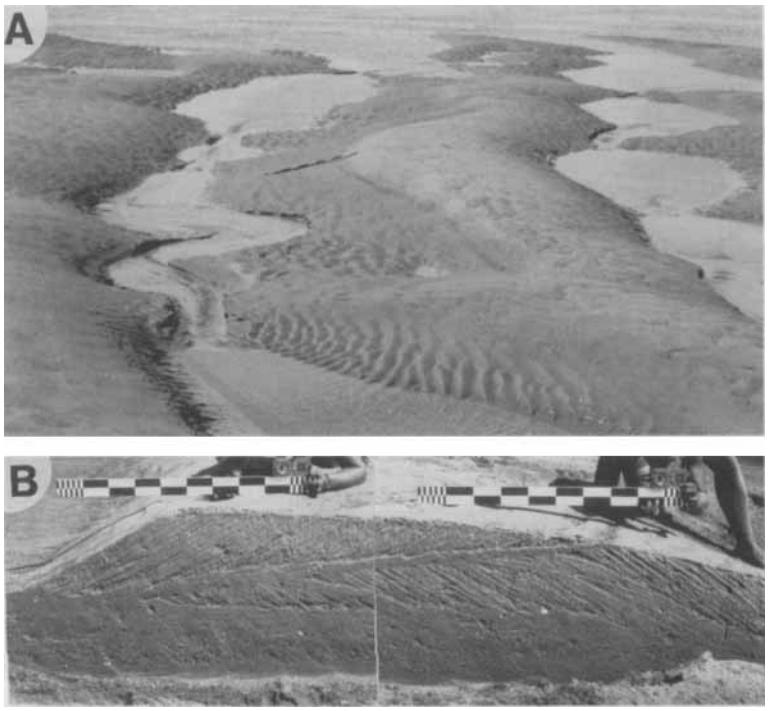

Fig. 21. (A) Small ebb cap on a flood-asymmetric megaripple; most of the flood stoss side remains exposed. Metre stick for scale. (B) Cross-section of flood-asymmetric megaripple with ebb cap which completely covers the flood stoss side. The flood core can be inferred from the convex-up profile of the ebb stoss side, which will become a reactivation surface. Two additional reactivation surfaces are visible within the bedform.

crossed by numerous, shallow channels which give the area a braided appearance (Swift & McMullen, 1968; Zaitlin, 1987; Dalrymple & Zaitlin, 1989). The local relief is subdued relative to zone 1 (Fig. 28A), and is generally less than 1·5–2 m, except in the vicinity of the Shubenacadie River thalweg. These sand flats occupy the elevation range between −8 m and −3 m (relative to mean high water). As the lateral extent of the sandy facies decreases eastwards (Fig. 3B), the number of minor channels becomes less until only the single main channel of the Salmon River is present beyond Lyons head (Fig. 2). In this inner area, which is designated zone 3, the axial sand facies occurs either as alternate bank-attached bars or tidal point bars (Zaitlin & Dalrymple, 1985a, b; Zaitlin, 1987; Dalrymple & Zaitlin, 1989). As in zone 2, the local relief is minor, with the sands generally not rising more than 1–1·5 m above the base of the channel.

Because of the headward convergence of the system (Fig. 3A) and the hydraulic sorting process described above (Fig. 13D), zones 2 and 3 are characterized by higher current speeds (Fig. 5) and finer sediment sizes (Figs 13C & 16) than zone 1: the dominant flood-current speeds generally exceed 2 ms^{-1}, and the mean sand size is fine or very fine sand, except near the tidal limit where fluvially transported coarse sand and gravel occurs (Zaitlin, 1987; Dalrymple & Zaitlin, 1989). These high current speeds, the fine sand size and the relatively shallow depths at the time of the maximum current speeds (generally <2–3 m), cause upper-flow-regime, plane-bed conditions to prevail throughout most of zones 2 and 3 (Fig. 13E; Dalrymple *et al.*, 1982; Zaitlin, 1987). Dunes of various types occur only in small patches at the western end of zone 2 (Zaitlin, 1987), and locally in a narrow band at the edge of the upper-flow-regime sand flats where the current speed is slightly less (Dalrymple *et al.*, 1982). These bedforms occur in sand with mean sizes of 0·13–0·18 mm, and their limited distribution reflects the small range of current speeds at which dunes exist in fine sand (Harms *et al.*, 1982, Fig. 2-5). Current ripples are the stable bedform throughout the entire tidal cycle only on the adjacent mixed flats.

Because of the widespread upper-flow-regime con-

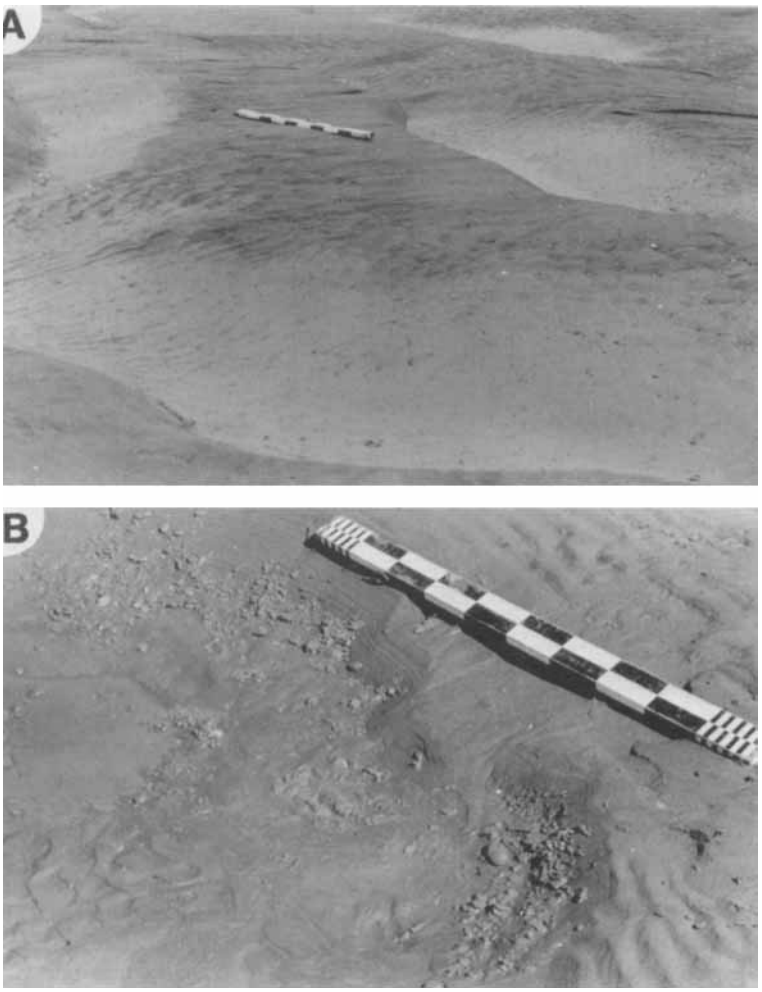

Fig. 22. (A) Mud drape (lighter tones) in troughs of 3-D megaripples. (B) Megaripple trough with mud pebbles eroded from a buried mud drape.

ditions (Fig. 13E), parallel lamination (Fig. 28B) is the most abundant structure in the axial sands of zones 2 and 3 (Dalrymple *et al.*, 1982; Zaitlin, 1987). The current, wave and/or combined-flow ripples which mantle all surfaces at low tide (Fig. 28A) form only a small fraction of the deposits, occurring as single ripple sets 10–30 mm thick, interspersed between sets of parallel lamination up to 0·3 m thick (Fig. 28B). Some larger-scale cross-bedding is also present; it is created by the few dunes that are present and/or by the margins of small channels which are oblique to the high-stage flow. At the edges of the high-energy sand flats, ripple cross-lamination and the number of mud drapes increase in abundance. Biogenic structures are not common, but they may occur in large numbers in local patches. The assemblage of burrow types is the same as that which occurs in the lower-energy parts of zone 1 (Fig. 25; Dewing, 1986; Dewing *et al.*, 1986; Zaitlin, 1987).

The mixed flats, mudflats and salt marshes which border the axial sands occupy the upper 1·5–4 m of the intertidal zone. Along the south side of zone 2, these facies occur in an unbroken, progradational succession up to 2 km wide (Figs 2 & 28C). By contrast, along the north shore where the main channel of the Salmon River lies close to the marsh (Fig. 2), a steep, erosional bank 3–4 m high separates the sands from the salt marsh. In zone 3, the confined

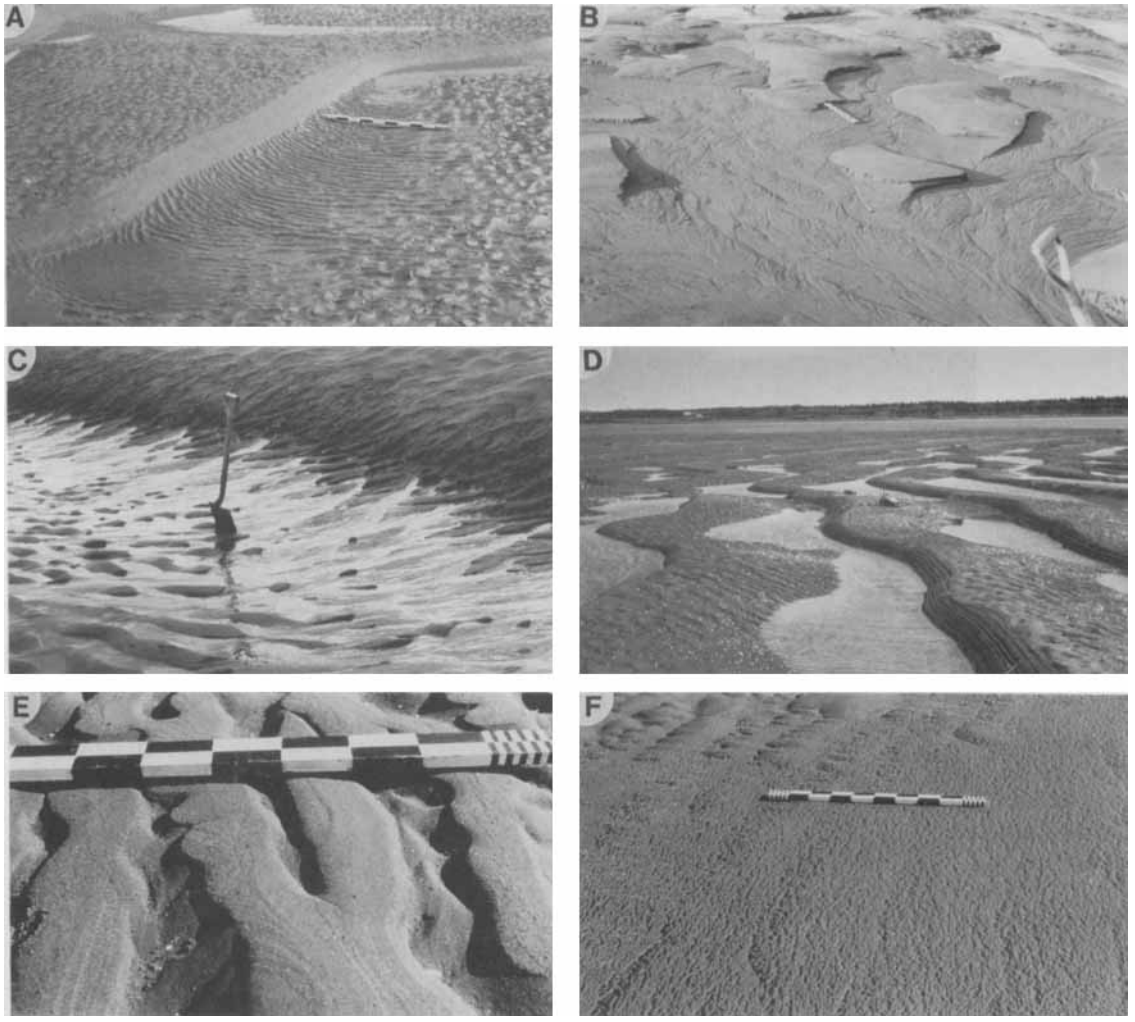

Fig. 23. Minor emergence features. (A) Late-ebb current ripples with orientations at a high angle to that of a 2-D megaripple. (B) Erosion of 3-D megaripples by water flowing along the bedform troughs. The rounded appearance of remnant megaripple crests is due to wave reworking during emergence. (C) Network of rills and a 'dewatering ramp' at toe of a sandwave lee face. (D) Water-level marks on a megaripple lee face. (E) Flat-topped ripples produced by wave action during emergence. (F) Adhesion ripples burying a field of ladder-back ripples (upper left corner).

nature of the system (Figs 2 & 3A,B), combined with frequent shifting of the thalweg, prevents the development of gradual, lateral transitions between facies. Instead, the sands are flanked by 2–4 terraces, each of which has a level surface composed of a single facies (Fig. 28D; Dalrymple & Makino, 1989; Dalrymple, Makino & Zaitlin, 1990). As the terraces build vertically, the sediment changes upward from sand to mud.

The sediments of the mixed flats are composed dominantly of sand in which ripple cross-lamination is the most abundant structure. Mud laminae, which are rarely thicker than 2–3 mm, become more abundant toward the mudflats and/or at higher elevations. In areas close to the sand flats, flasers are developed, whereas more continuous mud layers predominate near the mudflats. The mudflats are composed almost entirely of flat and wavy tidal bedding which consists of sand–mud couplets that range from < 1 to 50 mm thick (Fig. 28E; Dalrymple & Makino, 1989). The thicker sand layers commonly contain ripple cross-lamination whereas thinner ones are structureless;

Fig. 24. Ice-rafted block of salt-marsh sediment on Selmah Bar. The megarippled surface in the background has been smoothed by wave action during emergence.

additional details about the nature and origin of the tidal bedding are provided by Dalrymple & Makino (1989). Other structures present in the mudflats include minor amounts of lenticular bedding, soft-sediment deformation produced by ice (Dalrymple *et al.*, 1990), mud- and sand-filled desiccation cracks, and ice-crystal casts. Bioturbation generally increases in intensity upwards through the mixed flats and mudflats that are adjacent to zone 2, because the salinity at high tide is sufficient (Fig. 6) to support a moderately diverse and abundant infauna. As the salinity decreases headward, the diversity of benthic organisms and the overall degree of bioturbation decreases (cf. Fig. 28E; Dewing, 1986; Dewing *et al.*, 1986; Zaitlin, 1987). The burrow types present are characteristic of the *Skolithos* ichnofacies, and consist mainly of vertical to sub-vertical, simple, unbranched and U-shaped forms.

The salt marsh in the CB–SR estuary is generally confined to areas at or above the mean high water elevation, although colonization by grasses extends as much as 2 m below mean high water. The salt marsh sediments consist mainly of organic-rich silty muds with minor amounts of coarser ice-rafted material (Yeo & Risk, 1981). Massive bedding that retains only a vague horizontal fracture system is the main structure present (Fig. 28F). Desiccation cracks and rootlet casts are common. It should be noted that a sandy-gravel beach facies similar to that which occurs at the top of the foreshores in zone 1 is not present in zones 2 and 3.

The salt marsh, mudflats and mixed flats are dissected by sinuous, dendritic tidal gulleys that may reach 2–3 m in depth. The relief of those which are not connected to terrestrial streams generally increases seaward until near the salt-marsh–mudflat transition; from there the relief decreases outward as the sediments become sandier. Near the mixed-flat–sand-flat boundary, they either lose their identity entirely or merge with the broad, shallow channels of the sand flats. Lateral migration of the gulleys is negligible, and inclined, point-bar stratification is a minor constituent of the marginal facies.

VERTICAL FACIES MODEL

The rapid rise of the high-tide level (slightly more than 2 mm yr^{-1}; Scott & Greenberg, 1983) over the last 4000 years suggests that the CB–SR estuary is transgressive. However, the total volume of sediment estimated to be entering the system ($1{\cdot}15$–$9{\cdot}25 \times 10^6$ m^3 yr^{-1}; Amos & Long, 1980) would produce a layer 5–50 mm thick if it were spread uniformly over the entire subtidal and intertidal area headward of Noel Bay. Therefore, because the space created by the rise of the high-tide level is less than the sediment input, the system is *regressive* overall. Such regressive conditions may not have existed from 7000–4000 yr BP when the rate of rise of high water was faster (Fig. 4; Scott & Greenberg, 1983), and the rate of sediment input may have been less (Amos & Long, 1980). At this time, transgression probably occurred. The

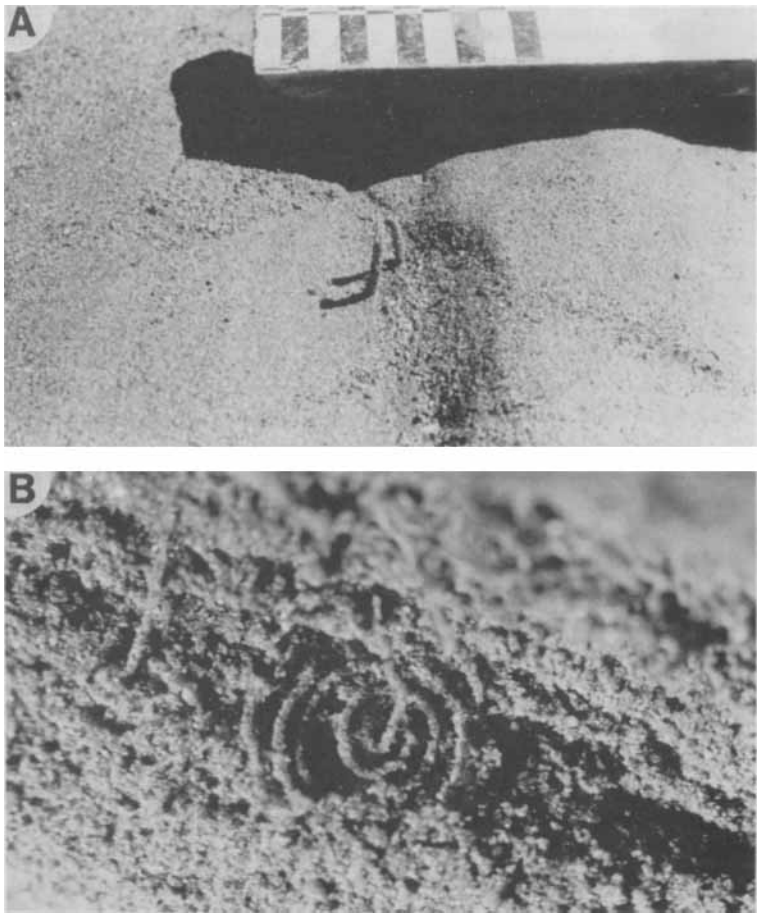

Fig. 25. (A) Agglutinated, vertical worm tube created by *Spiophanes wigleyi*. Scale in centimetres. (B) Horizontal spiral burrow of *Paraonis* sp. cast with epoxy resin as seen from above. Note vertical tube ascending from the centre of the spiral. Diameter of spiral is approximately 20 mm.

available information indicates, however, that the preserved record of the transgression is fragmentary; in most places the modern macrotidal sediments lie erosively on unrelated, older material. In the few places where transgressive successions exist, they consist of mudflat and/or salt-marsh sediments that are erosionally overlain by sand-bar deposits. As a result, a regressive facies model is developed below (cf. Knight & Dalrymple, 1975; Dalrymple, Knight & Middleton, 1985; Dalrymple & Zaitlin, 1989).

Unfortunately, there is no place in the complex where a complete, regressive section exists. In some areas adjacent to zone 2, regressive deposits up to 5–7 m thick are present, but these only contain sediments of the zone 2 sand flats, overlain by mixed-flat, mudflat and salt-marsh sediments. Therefore, in order to develop the ideal vertical succession which contains all of the facies zones, the headward facies have been projected seawards horizontally until they are superimposed on the zone 1 sand bars, using the elevations of the facies boundaries to determine the thickness of each facies (Fig. 29; Dalrymple *et al.*, 1985). Changes in the tidal range and sea-level during the time required for such a progradation to occur would, of course, cause the thicknesses to differ from those shown, but the general succession would remain unchanged. Strictly speaking, the model (Fig. 29) is specific to the CB–SR estuary; however, we will attempt to demonstrate in the Concluding Discussion that many of the essential features are duplicated in other macrotidal areas.

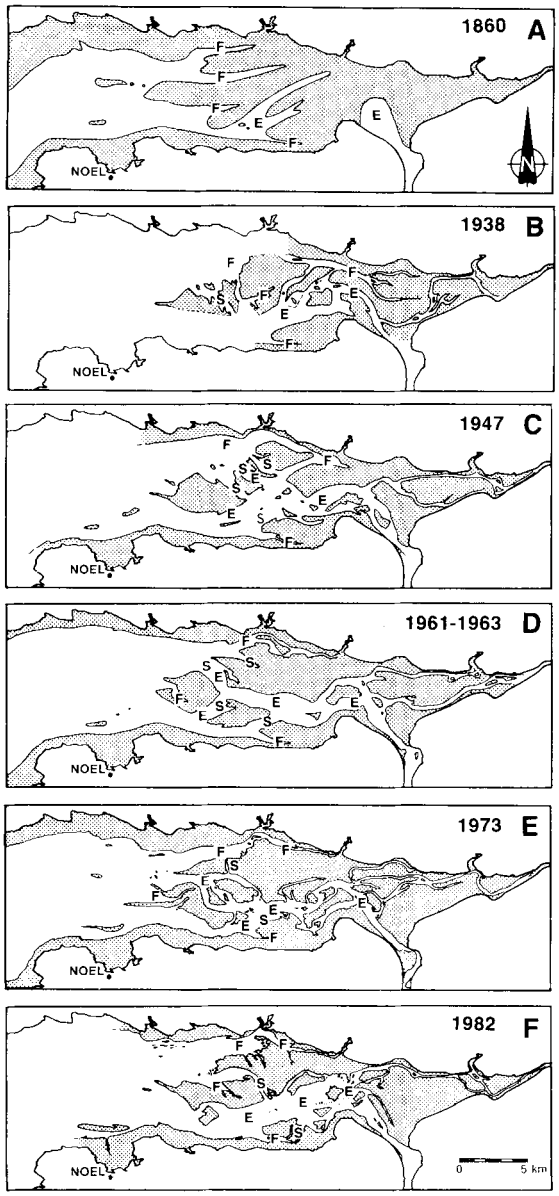

Fig. 26. Morphological evolution of zone 1 sand body between 1860 and 1982, with interpretation of the dominant transport directions: E–ebb-dominant, F–flood-dominant; S–major swatchway. Data sources: (A) British Admiralty Chart 353 (from Knight, 1980, Fig. 10.6A); (B)–(D) Canadian National Airphoto Library photographs (from Knight, 1980, Fig. 10.6B–D); (E) air photographs obtained by Middleton (from Dalrymple, 1977, Fig. 1.3; Knight, 1977, Fig. 3.15E); (F) air photographs obtained by first author.

The vertical facies succession for the CB–SR estuary (Fig. 29) is on the order of 20 m thick, based on the average high-tide water depth at the seaward end of zone 1 (Fig. 10). Its base is marked by a gravel lag which forms in zone 0 (Fig. 7), the channels between the zone 1 sand bars, and/or on the marginal foreshores (Fig. 8). The sand overlying this lag fines upward from the coarse sand in the bottom of the deeper channels, to the medium sand of the bar crests, and then to the fine sand of the zone 2 sand flats (Figs 13C & 16). These sands are overlain by the progressively more muddy sediments of the mixed flats, mudflats and salt marshes (Fig. 28C–F). Thus, the entire succession fines upward, and consists primarily of sands, with muddy sediments comprising only 20% of the total thickness (Fig. 29).

Slightly over half (10–13 m) of the total thickness is composed of sediment deposited on the elongate sand bars of zone 1 (Figs 2 & 29). These deposits, which will consist almost entirely of cross-bedded sands (Fig. 20), should be divisible into two major subfacies: the medium- to fine-grained sands of the central ebb channel; and the medium to coarse-grained sands of the flood-dominated areas (Figs 13C & 16). The ebb-channel sediments will occur within erosionally based channel(s), each of which is created as a swatchway gradually captures a greater share of the ebb flow and becomes wider and deeper (cf. Fig. 26). Such channels may not erode to the base of the estuary deposits because the ebb channel is generally shallower than the marginal flood channels (Figs 9 & 10). The ebb-channel deposits will consist mainly of ebb-orientated, trough cross-bedding, with minor amounts of flood cross-bedding (Fig. 20A). Progressively greater quantities of parallel lamination will be present in the headward (and thus higher) part of the ebb channel that is transitional with zone 2 (Figs 13E & 28A, B). The historical evidence suggests that only one ebb-channel unit will be present in the headward part of zone 1, whereas several may occur in the seaward part where most of the channel switching takes place (Fig. 26).

The dominant structure within the lower, coarser part of the flood-channel deposits will be inclined cross-bedding produced by sandwaves (Fig. 20C, D; Dalrymple, 1984a). Large-scale cross-beds (Fig. 20E, F) may also be present. Based on bedform heights, individual sandwave (co)sets might reach 3·5 m in thickness, but they will become thinner upwards as the bedforms become smaller. These structures may pass into planar–tabular cross-bedding (i.e. 2-D megaripples) in the highest part of the flood-dominant

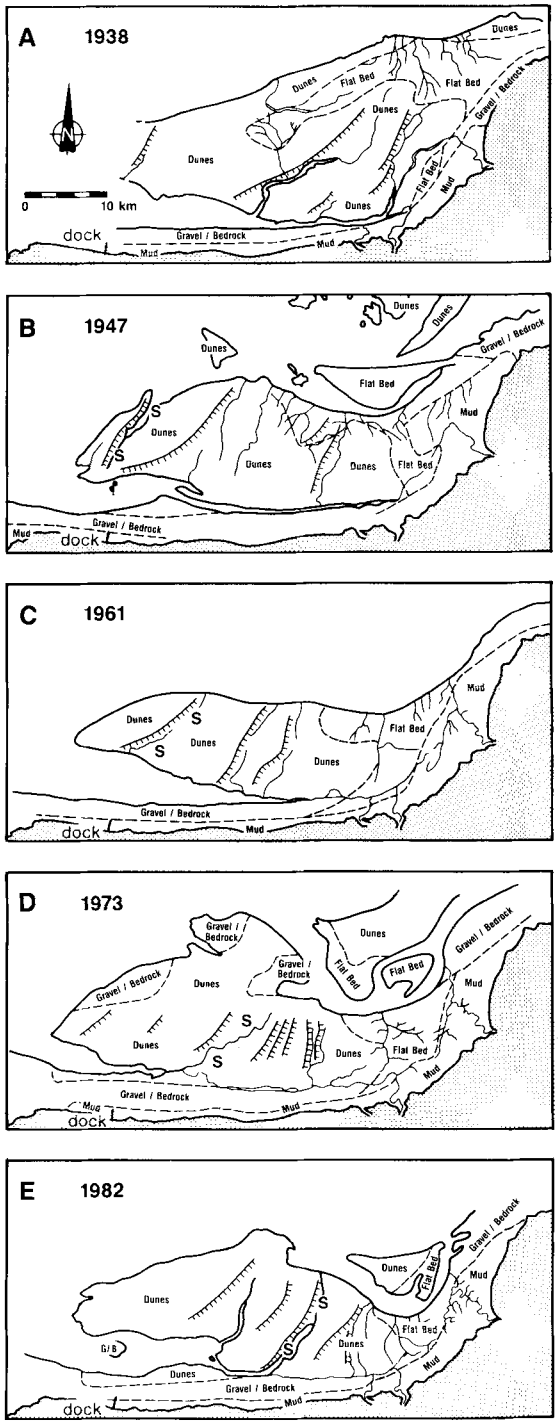

sands. The upper part of the flood-dominated areas may also contain significant amounts of sediment that was deposited on the western flank of the migrating swatchways (Fig. 29); such deposits are unlikely to extend to the base of the estuarine fill because swatchways are uncommon in the deeper, seaward half of zone 1 (Fig. 26). The sediment packages formed by the deeper swatchways will be several metres thick, and may either fine or coarsen upward (Fig. 17). Lateral-accretion surfaces may be present (Fig. 29), and will dip headward at low angles (2–5°), but with the dips directed obliquely outward from the axis of the estuary (Figs 11, 14 & 15). Although the swatchways move headward, the ebb dominance that characterizes their western margin (Figs 12C, 14B & 15B) causes the smaller structures to consist primarily of ebb-orientated, trough cross-bedding that is directed outward at a high angle (60–80°) to the length of the estuary. The margins of small swatchways (1–2 m deep) will contain structures which are similar to those in sandwaves (Fig. 20C–F), because both are formed by dunes that migrated down the depositional surface (Fig. 12A, B); the two may be distinguished, however, by the greater amount of along-strike flow in the swatchways (Fig. 12).

The available data do not permit an accurate estimate of the relative proportion of the ebb and flood deposits; however, flood-dominated areas (including the headward-migrating swatchways with their ebb cross-bedding) are more extensive than ebb-dominated regions (Figs 13A & 26) and it is possible that the deposits will show a similar flood predominance (Fig. 29). On the basis of cross-bedding alone, ebb and flood palaeocurrent directions may be nearly equally abundant.

The overlying sediments of the zone 2 sand flats will be composed of fine to very fine sand in which upper-flow-regime parallel lamination is the most abundant structure (Figs 28B & 29). Cut-and-fill structures produced by the shallow, braided channels (Fig. 2) may also be present. Ripple cross-lamination will be rare in most of this facies, but will increase in abundance as the sand-flat–mixed-flat boundary is

Fig. 27. Morphological and facies evolution of Selmah Bar. Data sources are the same as in Fig. 26. 'Dunes' refers to all large-scale bedforms. 'Flat Bed' denotes sandy areas lacking dunes; most of these areas are current rippled, but some in the main ebb channel may contain upper-flow-regime plane bed. G/B–gravel and/or bedrock. The lines with tick marks indicate the steep western margin of swatchways; S–the major swatchway whose migration is discussed in the text (see also Fig. 14).

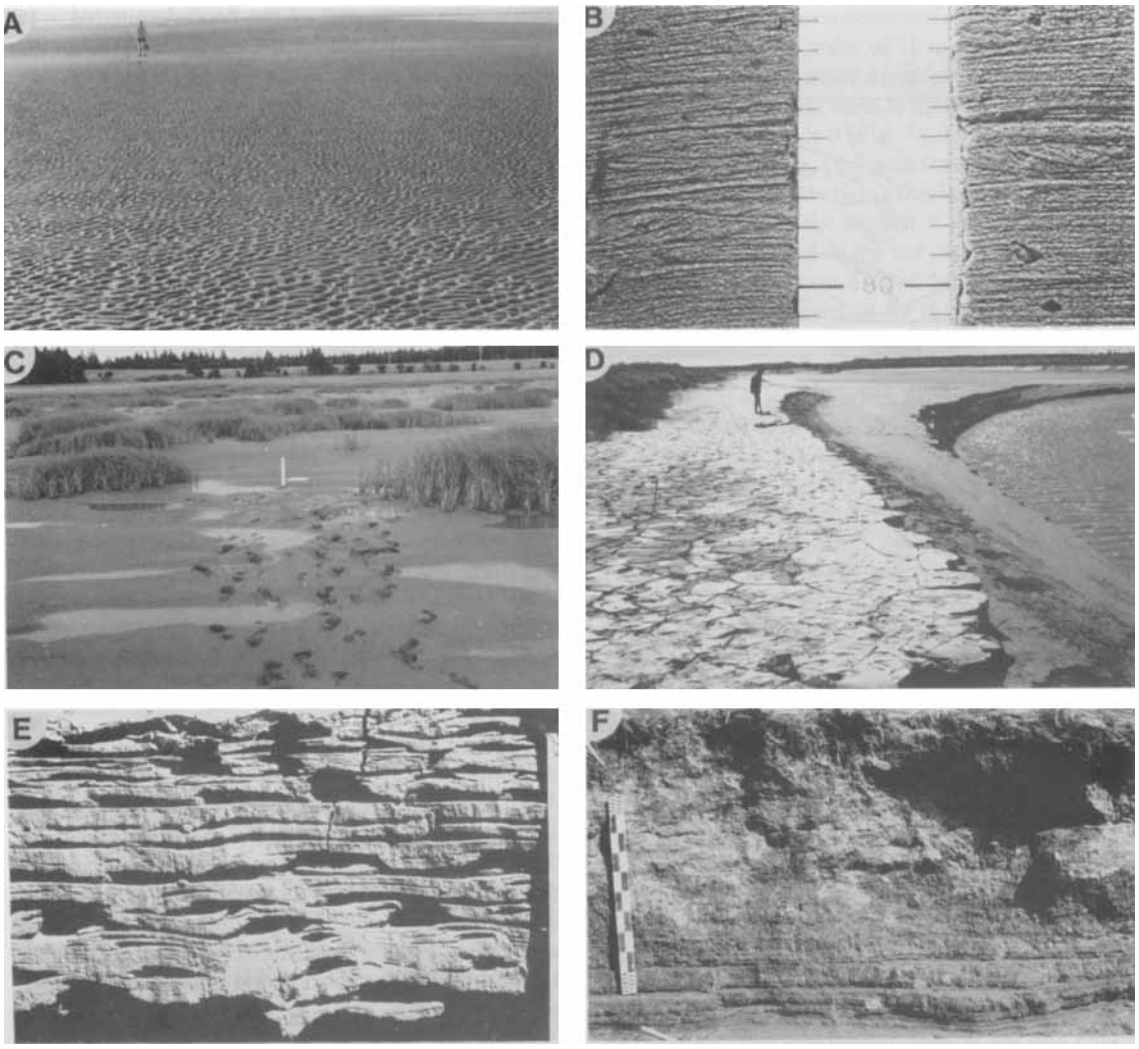

Fig. 28. (A) 'Featureless' surface of upper-flow-regime sand flat (zone 2) covered with late-ebb current ripples. (B) Portions of two cores from the zone 2 sand flats showing upper-flow-regime parallel lamination with minor ripple cross-lamination (flood flow to the left). Scale divisions are centimetres. (C) View landward over the mudflat–salt-marsh transition on the progradational flats, south side of zone 2 (Fig. 2). (D) Mudflat terraces along the Salmon River (zone 3). Note the active formation of an erosional scarp at the right side. (E) Lenticular and tidal bedding in the upper scarp in (D). Currents and waves have eroded the sand layers leaving cavities (flood flow to left). Note absence of bioturbation. The section shown is 0·27 m high. (F) Vertical transition from upper mudflat to salt marsh.

approached. These deposits will be overlain by a relatively typical, muddy tidal-flat sequence that passes upward from flaser-bedded sands of the mixed flats, through tidally bedded sands and muds of the mudflats (Fig. 28E; Dalrymple & Makino, 1989; Dalrymple *et al.*, 1990), to the root-mottled muds of the salt marsh (Figs 28F & 29). The degree of bioturbation will be moderate if the mudflats formed adjacent to zone 2, but minimal if they formed in zone 3 where the salinity is low (Fig. 6). Inclined, point-bar stratification will be rare. The thickness of these muddy deposits will be approximately 4 m. Note that a coarse-grained, beach facies is not included between the mudflat and salt-marsh sediments as is shown by Yeo & Risk (1981, Fig. 8; see also Weimer, Howard & Lindsay, 1982), because such a beach is not present

along the depositional margins of zones 2 and 3 (Fig. 28C, F; Terwindt, 1988).

The rather typical tidal-flat characteristics of the uppermost facies should allow the level of mean high water to be determined with reasonable confidence using the criteria described by many authors (e.g. Klein, 1971). By contrast, the low-tide level will be very difficult to identify because it occurs within the cross-bedded sands of the elongate sand bars. Only very careful searching for small-scale emergence features such as water-level marks, ripples with divergent orientations, rill marks and runoff micro-deltas (Klein, 1971; Clifton, 1983; Dalrymple, 1984b) will permit recognition of this level and determination of the tidal range.

CONCLUDING DISCUSSION

The preceding description of the Cobequid Bay–Salmon River estuarine complex has shown that sedimentation in such an environment must be viewed as an integrated system in which the flow dynamics (current speeds and net sediment transport pathways) create and interact with the bar-channel morphology to control the evolution of the morphology and the distribution of sediment sizes. These grain sizes together with the current speeds in turn determine the spatial distribution of bedform types and sedimentary structures. It is because all of these interacting variables are understood that we are able to develop a facies model (Fig. 29) which is considerably more detailed than any of the previous models for macrotidal environments (Knight & Dalrymple, 1975, Fig. 6-10; Coleman & Wright, 1975, Fig. 19; Galloway & Hobday, 1983, Fig. 6-17; Terwindt, 1988, Fig. 2). All of these models show the deposits of the elongate bars as an undifferentiated sand body composed of simple cross-bedding, and only the model presented by Knight & Dalrymple (1975) contains a separate (but incorrectly represented) unit for the zone 2 sand flats. It remains, however, to evaluate the generality of the new model (Fig. 29).

A detailed comparison of the study area with other macrotidal settings is beyond the scope of this paper, but the important similarities and differences will be noted. For the sake of brevity, our comments are restricted to modern estuaries with tidal ranges greater than 10 m.

A headward-fining trend is a common feature of the axial sands in the outer part of all macrotidal estuaries for which adequate textural data are avail-

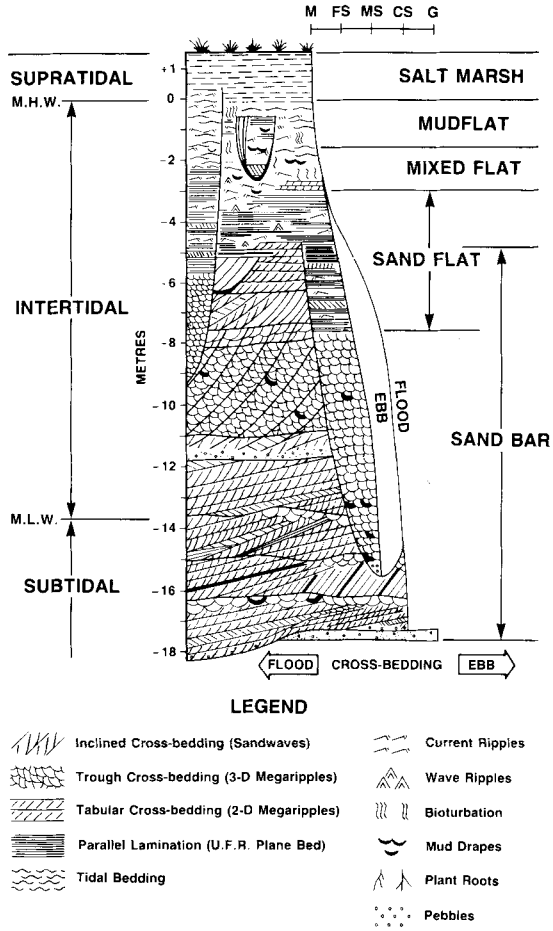

Fig. 29. Vertical facies model for the Cobequid Bay–Salmon River estuary (modified after Dalrymple *et al.*, 1985, Fig. 2). The right-hand margin of the schematic section gives the approximate grain size: M–mud, FS–fine sand, MS–medium sand, CS–coarse sand, G–gravel. M.H.W. and M.L.W.–mean high and low water. U.F.R.–upper flow regime.

able (i.e. the CB–SR estuary—this study; the Avon River, Bay of Fundy—Lambiase, 1977, 1980a, b; and the Bristol Channel–Severn River, England—Hamilton, 1979, 1982). The headward-fining trend in the first two examples is ascribed to the hydraulic sorting mechanism associated with the headward termination of the major flood channels (Fig. 13D; Lambiase, 1977, 1980a, b; this study), but Hamilton (1979, 1982) has suggested that this trend exists in the Severn estuary because the fine sand at its head is the most readily entrained and rapidly transported size fraction, the implication being that insufficient time has elapsed for the coarser sizes to reach the inner estuary. Sediment tracer studies in Cobequid Bay have shown,

however, that such grain sizes can be transported several tens of kilometres (net) in a few hundred years (Dalrymple, 1977). Thus, this coarse material can move headward sufficiently rapidly to outpace any transgression, and, as a result, Hamilton's (1979, 1982) explanation is unlikely to be correct. On the other hand, the most abrupt decrease in grain size in the Severn estuary occurs at the headward end of the flood-dominated, Newport Channel (Parker & Kirby, 1982; Harris & Collins, 1985), and it is concluded that the hydraulic exclusion process is probably responsible. Therefore, because the headward termination of flood-dominant channels is a universal characteristic of estuaries (Robinson, 1960), this sediment-sorting mechanism and the headward-fining trend which it produces are probably present in all macrotidal estuaries. Note, however, that such a trend will not continue into the fluvially dominated, innermost part of the estuary if the river supplies coarse sediment (Dalrymple & Zaitlin, 1989).

Most macrotidal estuaries also display a pronounced, funnel-shaped geometry (Wright *et al.*, 1973), which causes them to be hypersynchronous (i.e. the tidal current speeds reach a maximum part way along the length of the estuary; Fig. 5; Salomon & Allen, 1983; Nichols & Biggs, 1985). This distribution of current speeds, together with the headward-fining and shallowing trends, leads to the development of a common, longitudinal facies pattern. Elongate, tidal sand bars (zone 1) are widely known to be a general feature of the seaward end of macrotidal embayments (Hayes, 1975; Harris, 1988), and are covered by dunes of various types in all cases (Wright, Coleman & Thom, 1975; Dalrymple *et al.*, 1978; Lambiase, 1980a, b; Harris & Collins, 1985). Headward of these bars, upper-flow-regime conditions have been documented in the Cobequid Bay, Avon River, Severn River and Cook Inlet estuaries (Hamilton, 1979; Lambiase, 1980a, b; Bartsch-Winkler & Ovenshine, 1984), and horizontally laminated fine sands (and upper-flow-regime conditions?) characterize the estuarine channels in the Colorado River delta (Meckel, 1975). Therefore, all of these estuaries should develop similar, upward-fining, regressive successions in which cross-bedded medium to coarse sand is overlain by parallel-laminated fine sand (Fig. 29). Muddy, tidal-flat sediments cap the estuarine deposits in all of these areas.

Within the framework of the fundamental similarities discussed above, numerous local differences do occur. One of the most important of these is the depth of water into which the estuarine complex progrades, as this determines the maximum thickness of the deposits. Thus, the complete succession in both the Severn River–Bristol Channel estuary (Hamilton, 1979; Parker & Kirby, 1982) and Cook Inlet (Bouma, Hampton & Orlando, 1977; Bartsch-Winkler & Ovenshine, 1984) might exceed 40 m in thickness. Such greater water depths may also cause the cross-bedding to plane-bed facies boundary to shift to greater water depths, as dunes are largely confined to the subtidal zone in both of these localities (Bartsch-Winkler & Ovenshine, 1984; Harris & Collins, 1985). As a result, the low-tide elevation will occur at a relatively higher elevation in the succession in these areas than it does in the CB–SR estuary (Fig. 29).

The relative abundance of the cross-bedded and parallel-laminated facies may also differ between estuaries because of differences in the relative abundance of the various sand sizes. For example, medium and coarse sand is not abundant in Chignecto Bay, Bay of Fundy (Fig. 1B; Amos & Zaitlin, 1985); consequently, the elongate sand bars there average only 2–3 m in thickness and do not extend into the intertidal zone. A similar deficiency of the coarser sand sizes might also contribute to the restriction of dunes to the subtidal portions of the Bristol Channel and Cook Inlet. In such cases, the finer-grained sediments of facies zones 2 and 3 (Fig. 29) may form a greater proportion of the entire succession.

Estuaries also differ with respect to the size and shape of the valley in which they lie. In the CB–SR estuary, the valley is relatively narrow and straight sided (Fig. 3A, B) so that zone 1 is confined by the valley walls and is bordered by erosional or non-depositional foreshores (Figs 2 & 8). In the Severn River–Bristol Channel and South Alligator River areas, by contrast, the valley width is sufficiently great in zone 1 that the sand bars are flanked by thick accumulations of mudflat and salt-marsh sediment (Allen & Rae, 1988; Woodroffe *et al.*, 1985a, b, 1989). In this situation, *lateral* infilling of zone 1 might produce a vertical succession somewhat different from that proposed here (Fig. 29), in that the upper-flow-regime sand flats would probably be absent. Longitudinal progradation in both areas would, however, generate deposits similar to those in the CB–SR estuary (Fig. 29), because of the fundamental hydrodynamic and sedimentological similarities noted above.

ACKNOWLEDGMENTS

This study was initiated when R.W.D. and R.J.K.

were graduate students under the supervision of G.V.M. The early stages of this work were supported by grants to G.V.M. from the National Research Council of Canada and the Department of Energy, Mines and Resources (Canada), and to R.J.K. from the Department of Energy Mines and Resources and the Geological Society of America (GSA). Subsequent work by R.W.D. and B.A.Z. has been financed by grants to R.W.D. from the Natural Sciences and Engineering Research Council of Canada, the Advisory Research Committee of Queen's University, Imperial Oil Ltd, Gulf Canada Ltd, Mobil Oil Ltd, Shell Oil Ltd and Canterra Energy Ltd. B.A.Z. also acknowledges a grant from GSA. The support provided by the Bedford Institute of Oceanography, and especially by C. L. Amos, at various times throughout the project is acknowledged with particular thanks, as is the generally uncomplaining effort of many assistants over the years. The drafting and photographic work was ably performed by Ela Rusak Mazur (Queen's University) and Esso Resources Canada Ltd. The comments provided by the journal reviewers were helpful in making the presentation more concise.

REFERENCES

ALLEN, J.R.L. (1982) Mud drapes in sand-wave deposits: physical model with application to the Folkestone Beds (Early Cretaceous, southeast England). *Phil. Trans. R. Soc.*, **A306**, 291–345.

ALLEN, J.R.L. & RAE, J.E. (1988) Vertical salt-marsh accretion since the Roman period in the Severn estuary, southwest Britain. *Mar. Geol.*, **83**, 225–235.

AMOS, C.L. (1978) The post glacial evolution of the Minas Basin, N.S.: a sedimentological interpretation. *J. sedim. Petrol.*, **48**, 965–982.

AMOS, C.L. & ALFOLDI, T.T. (1979) The determination of suspended sediment concentration in a macrotidal system using LANDSAT data. *J. sedim. Petrol.*, **49**, 159–174.

AMOS, C.L., BUCKLEY, D.E., DABORN, G.R., DALRYMPLE, R.W., MCCANN, S.B. & RISK, M.J. (1980) Geomorphology and Sedimentology of the Bay of Fundy. *Guidebk. Geol. Ass. Canada, Annual Meeting, Halifax, Trip 23*, 82 pp.

AMOS, C.L. & LONG, B.F.N. (1980) The sedimentary character of the Minas Basin, Bay of Fundy. In: *The Coastline of Canada* (Ed. by S.B. McCann), pp. 123–152. *Paps Geol. Surv. Canada*, **80–10**, 437 pp.

AMOS, C.L. & MOSHER, D.C. (1985) Erosion and deposition of fine-grained sediments from the Bay of Fundy. *Sedimentology*, **32**, 815–832.

AMOS, C.L. & ZAITLIN, B.A. (1985) The effect of changes in tidal range on a sublittoral macrotidal sequence, Bay of Fundy, Canada. *Geo-Mar. Lett.*, **4**, 161–169.

ASHLEY, G.M., et al. (1990) Classification of large-scale subaqueous bedforms: a new look at an old problem. *J. sedim. Petrol.*, **60**, 160–172.

ATPEMC (Atlantic Tidal Power Engineering and Management Committee) (1969) *Report to Atlantic Tidal Power Programming Board on Feasibility of Tidal Power Development in the Bay of Fundy*. Halifax.

BARTSCH-WINKLER, S. (1988) Cycle of earthquake-induced aggradation and related tidal channel shifting, upper Turnagain Arm, Alaska, USA. *Sedimentology*, **35**, 621–628.

BARTSCH-WINKLER, S. & OVENSHINE, A.T. (1984) Macrotidal subarctic environment of Turnagain and Knik Arms, Upper Cook Inlet, Alaska: sedimentology of the intertidal zone. *J. sedim. Petrol.*, **54**, 1221–1238.

BLEAKNEY, J.S. (1985) A sea-level scenario for Minas Basin. In: *Effects of Changes in Sea Level and Tidal Range in the Gulf of Maine–Bay of Fundy System* (Ed. by G.R. Daborn), pp. 123–125. *Pubs Acadia Centre Estuarine Research*, **1**, 133 pp.

BOUMA, A.H., HAMPTON, M.A. & ORLANDO, R.C. (1977) Sand waves and other bedforms in lower Cook Inlet, Alaska. *Mar. Geotechnol.*, **2**, 291–308.

BUJAK, J.P. & DONOHOE, H.V., JR. (1980) Geological Highway Map of Nova Scotia. *Spec. publs Atlantic Geoscience Soc.*, **1**, Halifax.

CANADIAN HYDROGRAPHIC SERVICE (1984) *Canadian Tide and Current Tables, Vol. 1, Atlantic Coast and Bay of Fundy*. Dept. Environment, Ottawa, 53 pp.

CASTON, V.N.D. & STRIDE, A.H. (1970) Tidal sand movement between some linear sand banks in the North Sea off northeast Norfolk. *Mar. Geol.*, **9**, M38–42.

CLIFTON, H.E. (1982) Estuarine deposits. In: *Sandstone Depositional Environments* (Ed. by P.A. Scholle & D. Spearing), pp. 179–189. *Am. Ass. Petrol. Geol., Tulsa*, 410 pp.

CLIFTON, H.E. (1983) Discrimination between subtidal and intertidal facies in Pleistocene deposits, Willapa Bay, Washington. *J. sedim. Petrol.*, **53**, 353–369.

COLEMAN, J.M. & WRIGHT, L.D. (1975) Modern river deltas: variability of process and sand bodies. In: *Deltas: Models for Exploration* (Ed. by M. L. Broussard), pp. 99–149. Houston Geol. Soc., Houston, 555 pp.

DALRYMPLE, R.W. (1977) *Sediment dynamics of macrotidal sand bars, Bay of Fundy*. PhD thesis, McMaster University, Hamilton, 635 pp.

DALRYMPLE, R.W. (1979) Wave-induced liquefaction: a modern example from the Bay of Fundy. *Sedimentology*, **26**, 835–844.

DALRYMPLE, R.W. (1980) Size populations and their transport behaviour over bedforms. *Geol. Soc. Am. Abstr. with Progs.*, **12**, 30.

DALRYMPLE, R.W. (1984a) Morphology and internal structure of sandwaves in the Bay of Fundy. *Sedimentology*, **31**, 365–382.

DALRYMPLE, R.W. (1984b) Runoff microdeltas: a potential emergence indicator in cross-bedded sandstones. *J. sedim. Petrol.*, **54**, 825–830.

DALRYMPLE, R.W., AMOS, C.L. & MCCANN, S.B. (1982) Beach and Nearshore Depositional Environments of the Bay of Fundy and Southern Gulf of St. Lawrence. *Guidebks Int. Ass. Sedimentol. 11th Congr., Hamilton, Excursion 6A*, 116 pp.

DALRYMPLE, R.W., KNIGHT, R.J. & LAMBIASE, J.J. (1978) Bedforms and their hydraulic stability relationships in a

tidal environment, Bay of Fundy, Canada. *Nature*, **275**, 100–104.

DALRYMPLE, R.W., KNIGHT, R.J. & MIDDLETON, G.V. (1975) Intertidal sand bars in Cobequid Bay (Bay of Fundy). In: *Estuarine Research* (Ed. by L. E. Cronin), II, pp. 293–307. Academic Press, New York, 587 pp.

DALRYMPLE, R.W., KNIGHT, R.J. & MIDDLETON, G.V. (1985) Facies distribution and sequences in a sandy macrotidal estuary, Cobequid Bay–Salmon River estuary, Bay of Fundy, Canada. *Abstrs Int. Ass. Sedimentol., Symp. Modern and Ancient Clastic Tidal Deposits*, Utrecht, 57–60.

DALRYMPLE, R.W. & MAKINO, Y. (1989) Description and genesis of tidal bedding in the Cobequid Bay–Salmon River estuary, Bay of Fundy, Canada. In: *Sedimentary Facies in the Active Plate Margin* (Ed. by A. Taira & F. Masuda), pp. 151–177. Terra Scientific, Tokyo, 732 pp.

DALRYMPLE, R.W., MAKINO, Y. & ZAITLIN, B.A. (1990) Temporal and spatial patterns of mudflat sedimentation in a macrotidal estuary, Cobequid Bay–Salmon River estuary, Bay of Fundy. In: *Clastic Tidal Sedimentology* (Ed. by R. A. Rahmani, D. G. Smith, G. E. Reinson & B. A. Zaitlin), *Mem. Can. Soc. petrol. Geol.*, **16**, in press.

DALRYMPLE, R.W. & ZAITLIN, B.A. (1985) Sedimentation in the macrotidal, Cobequid Bay–Salmon River estuary. In: *Glaciers, Sediment and Sea Level; Northern Bay of Fundy, N.S.* (Ed. by R. Grant). *Guidebk. 14th Arctic Workshop on Arctic Land–Sea Interaction, Appendix I*, pp. A1–A6. Dartmouth, 36 pp.

DALRYMPLE, R.W. & ZAITLIN, B.A. (1989) Tidal sedimentation in the macrotidal, Cobequid Bay–Salmon River estuary, Bay of Fundy. *Can. Soc. petrol. Geol., Field Guide, 2nd. Int. Res. Symp. Clastic Tidal Deposits, Calgary, Alberta*, 84 pp.

DAVIES, J.L. (1964) A morphogenetic approach to world shorelines. *Zeit. fur Geomorph.*, **8**, 127–142.

DAWSON, W.B. (1917) *Tides at the Head of the Bay of Fundy*. Dept. Naval Serv., Ottawa, 34 pp.

DEWING, K. (1986) *Organisms zonation in a macrotidal estuary, Cobequid Bay–Salmon River, Bay of Fundy, Nova Scotia, Canada*. BSc thesis, Queen's University, Kingston, 88 pp.

DEWING, K.E., ZAITLIN, B.A., NARBONNE, G.M. & DALRYMPLE, R.W. (1986) Zonation of trace-producing organisms from the Cobequid Bay–Salmon River estuary, Bay of Fundy. *Geol. Ass. Canada Progr. with Abstr.*, **11**, 63.

FEATHERSTONE, R.P. & RISK, M.J. (1977) Effect of tube-building polychaetes on intertidal sediments of the Minas Basin, Bay of Fundy. *J. sedim. Petrol.*, **47**, 446–450.

GALLOWAY, W.E. & HOBDAY, D.K. (1983) *Terrigenous Clastic Depositional Systems—Applications to Petroleum, Coal and Uranium Exploration*. Springer-Verlag, New York, 423 pp.

GRANT, D.R. (1985) Glaciers, sediment and sea level; Northern Bay of Fundy, Nova Scotia. *Guidebk. 14th Arctic Workshop on Arctic Land–Sea Interaction, Dartmouth, Nova Scotia*, 36 pp.

GREENBERG, D.A. (1979) A numerical model investigation of tidal phenomena in the Bay of Fundy and Gulf of Maine. *Mar. Geodesy*, **2**, 161–187.

GREENBERG, D.A. & AMOS, C.L. (1983) Suspended sediment transport and deposition modeling in the Bay of Fundy, Nova Scotia—a region of potential tidal power development. *Can. J. Fish. Aquatic Sci.*, **40**, 20–34.

HAMILTON, D. (1979) The high energy, sand and mud regime of the Severn estuary, S.W. Britain. In: *Tidal Power and Estuary Management* (Ed. by R. T. Severn, D. Dineley & L. E. Hawker), pp. 162–172. *Colston Paps*, **30**, 266 pp.

HAMILTON, D. (1982) Discussion. In: *Severn Barrage* (Ed. by Inst. Civ. Engrs), pp. 210–212. Thomas Telford, London.

HARMS, J.C., SOUTHARD, J.B. & WALKER, R.G. (1982) Structures and sequences in clastic rocks. *Short Courses Soc. econ. Paleont. Miner., Tulsa*, **9**.

HARRIS, P.T. (1988) Large-scale bedforms as indicators of mutually evasive sand transport and the sequential infilling of wide-mouthed estuaries. *Sediment. Geol.*, **57**, 273–298.

HARRIS, P.T. & COLLINS, M.B. (1985) Bedform distribution and sediment transport paths in the Bristol Channel and Severn Estuary, U.K. *Mar. Geol.*, **62**, 153–166.

HAYES, M.O. (1975) Morphology of sand accumulations in estuaries: an introduction to the symposium. In: *Estuarine Research* (Ed. by L. E. Cronin), II, pp. 3–22. Academic Press, New York, 587 pp.

HAYES, M.O. (1979) Barrier island morphology. In: *Barrier Islands from the Gulf of St. Lawrence to the Gulf of Mexico* (Ed. by S. P. Leatherman), pp. 1–28. Academic Press, New York, 325 pp.

HENNIGAR, T.W. (1972) Hydrogeology of the Truro area, Nova Scotia. *Repts N.S. Dept. Mines Groundwater Sect.*, **72–1**, 127 pp.

HOUBOLT, J.J. (1968) Recent sediments in the southern bight of the North Sea. *Geologie Mijnb.*, **47**, 245–273.

HUBERT, J.F. & MERTZ, K.A. (1980) Eolian dune field of Late Triassic age, Fundy Basin, Nova Scotia. *Geology*, **8**, 516–519.

HUTHNANCE, J.M. (1982) On one mechanism forming linear sandbanks. *Estuarine, Coastal and Shelf Sci.*, **14**, 79–99.

KEPPIE, J.D. (1982) The Minas geofracture. In: *Major Structural Zones and Faults of the Northern Appalachians* (Ed. by P. St.-Julien & J. Beland), pp. 263–280. *Spec. paps geol. Ass. Canada*, **24**, 280 pp.

KLEIN, G.DEV. (1963) Bay of Fundy intertidal zone sediments. *J. sedim. Petrol.*, **33**, 844–854.

KLEIN, G.DEV. (1970) Depositional and dispersal dynamics of intertidal sand bars. *J. sedim. Petrol.*, **40**, 1095–1127.

KLEIN, G.DEV. (1971) A sedimentary model for determining paleotidal range. *Bull. geol. Soc. Am.*, **82**, 2585–2592.

KNIGHT, R.J. (1977) *Sediments, bedforms and hydraulics in a macrotidal environment, Cobequid Bay (Bay of Fundy)*. PhD thesis, McMaster University, Hamilton, 693 pp.

KNIGHT, R.J. (1980) Linear sand bar development and tidal current flow in Cobequid Bay (Bay of Fundy), Nova Scotia. In: *The Coastline of Canada* (Ed. by S. B. McCann), pp. 153–180. *Paps Geol. Surv. Canada*, **80–10**, 437 pp.

KNIGHT, R.J. & DALRYMPLE, R.W. (1975) Intertidal sediments from the south shore of Cobequid Bay, Bay of Fundy, Nova Scotia, Canada. In: *Tidal Deposits: A Casebook of Recent Examples and Fossil Counterparts* (Ed. by R. N. Ginsburg), pp. 47–55. Springer-Verlag, New York, 428 pp.

KNIGHT, R.J. & DALRYMPLE, R.W. (1976) Winter conditions in a macrotidal environment, Cobequid Bay, Nova Scotia. *Rev. Geogr. Montreal*, **XXX**, 65–85.

LAMBIASE, J.J. (1977) *Sediment dynamics in the macrotidal Avon River estuary, Nova Scotia*. PhD thesis, McMaster University, Hamilton, 415 pp.

LAMBIASE, J.J. (1980a) Hydraulic control of grain-size

distributions in a macrotidal estuary. *Sedimentology*, **27**, 433–446.

LAMBIASE, J.J. (1980b) Sediment dynamics in the macrotidal Avon River estuary, Bay of Fundy, Nova Scotia. *Can. J. Earth Sci.*, **17**, 1628–1641.

LARSONNEUR, C. (1975) Tidal deposits, Mont Saint-Michel Bay, France. In: *Tidal Deposits: A Casebook of Recent Example and Fossil Counterparts* (Ed. by R. N. Ginsburg), pp. 21–30. Springer-Verlag, New York, 428 pp.

LARSONNEUR, C. (1988) *La Baie du Mont Saint-Michel: un Model de Sedimentation en Zone Temperee*. Univ. de Caen, Caen, 85 pp.

LINCOLN, J.M. & FITZGERALD, D.M. (1988) Tidal distortions and flood dominance at five small tidal inlets in southern Maine. *Mar. Geol.*, **82**, 133–148.

MAHER, A.J. (1986) *A statistical analysis of grain size distribution, Cobequid Bay–Salmon River estuary (Bay of Fundy), Nova Scotia*. BSc thesis, Queen's University, Kingston 120 pp.

MECKEL, L.D. (1975) Holocene sand bodies in the Colorado River delta area, northern Gulf of California. In: *Deltas: Models for Exploration* (Ed. by M. L. Broussard), pp. 87–98. Houston Geol. Soc., Houston, 555 pp.

MIDDLETON, G.V. (1976) Hydraulic interpretation of sand size distributions. *J. Geol.*, **84**, 405–426.

MYRICK, R.M. & LEOPOLD, L.B. (1963) Hydraulic geometry of a small tidal estuary. *Prof. paps US geol. Surv.*, **422-B**, 18 pp.

NICHOLS, M.M. & BIGGS, R.B. (1985) Estuaries. In: *Coastal Sedimentary Environments*, 2nd edn (Ed. by R. A. Davis Jr), pp. 77–186. Springer-Verlag, New York, 716 pp.

PARKER, W.R. & KIRBY, R. (1982) Sources and transport patterns of sediment in the inner Bristol Channel and Severn Estuary. In: *Severn Barrage* (Ed. by Inst. Civ. Engrs), pp. 181–194. Thomas Telford, London, 240 pp.

PILLSBURY, G.B. (1939) Tidal Hydraulics. *Prof. paps US Corps of Engrs*, **34**, 281 pp.

PRITCHARD, D.W. & CARTER, H.H. (1971) Estuarine circulation patterns. In: *The Estuarine Environment* (Ed. by J. R. Shubel), pp. 1–17. Am. geol. Inst., Washington.

RISK, M.J. & TUNNICLIFFE, V.J. (1978) Intertidal spiral burrows: *Paraonis fulgens* and *Spiophanes wigley* in the Minas Basin, Bay of Fundy. *J. sedim. Petrol.*, **48**, 1287–1292.

RISK, M.J. & YEO, R.K. (1980) Animal–sediment relationships in the Minas Basin, Bay of Fundy. In: *The Coastline of Canada* (Ed. by S. B. McCann), pp. 189–194. *Paps Geol. Surv. Canada*, **80–10**, 437 pp.

ROBINSON, A.H.W. (1960) Ebb-flood channel systems in sandy bays and estuaries. *Geography*, **45**, 183–199.

ROLAND, A.E. (1982) *Geological Background and Physiography of Nova Scotia*. Nova Scotia Inst. Sci., Halifax, 311 pp.

SALOMON, J.C. & ALLEN, G.P. (1983) Roles sedimentologique de la maree dans les estuaries a fort marnage. *Notes and Memoires, Compagnie Francaise des Petroles*, **18**, 35–44.

SCOTT, D.B. & GREENBERG, D.A. (1983) Relative sea-level rise and tidal development in the Fundy tidal system. *Can. J. Earth Sci.*, **20**, 1554–1564.

STEVENS, G.R. (1980) Mesozoic vulcanism and structure—Northern Bay of Fundy region, Nova Scotia. *Guidebks Geol. Ass. Canada, Annual Meeting, Halifax, Trip* **8**, 41 pp.

SWIFT, D.J.P. & BORNS, H.W. (1967) Genesis of the raised fluviomarine outwash terrace, north shore of the Minas Basin, N.S.—a preliminary report. *Marit. Sed.*, **3**, 17–23.

SWIFT, D.J.P. & LYALL, A.K. (1968) Origin of the Bay of Fundy: an interpretation from sub-bottom profiles. *Mar. Geol.*, **6**, 331–343.

SWIFT, D.J.P. & MCMULLEN, R.M. (1968) Preliminary studies of intertidal sand bodies in the Minas Basin, Bay of Fundy, Nova Scotia. *Can. J. Earth Sci.*, **5**, 175–183.

TERWINDT, J.H.J. (1981) Origin and sequences of sedimentary structures in inshore mesotidal deposits of the North Sea. In: *Holocene Marine Sedimentation in the North Sea Basin* (Ed. by S.-D. Nio, R. T. E. Shuttenhelm & Tj. C. E. van Weering), pp. 4–26. *Spec. publs Int. Ass. Sedimentol.*, **5**, 515 pp.

TERWINDT, J.H.J. (1988) Palaeo-tidal reconstructions of inshore tidal depositional environments. In: *Tide-Influenced Sedimentary Environments and Facies* (Ed. by P. L. deBoer, A. vanGelder & S.-D. Nio), pp. 233–263. Boston, Reidel Publ. Co., 530 pp.

VAIL, P.R., MITCHUM, R.M., JR. & THOMPSON, S., III (1977) Seismic stratigraphy and global changes in sea level, part 4: global cycles of relative changes in sea level. *Mem. Am. Ass. petrol. Geol.*, **26**, 83–97.

WEIMER, R.J., HOWARD, J.D. & LINDSAY, D.R. (1982) Tidal flats and associated tidal channels. In: *Sandstone Depositional Environments* (Ed. by P. A. Scholle & D. Spearing), pp. 191–245. Am. Ass. petrol. Geol., Tulsa, 410 pp.

WIGHTMAN, D.M. (1980) *Late Pleistocene glacio-fluvial and glacio-marine sediments on the north side of Minas Basin, Nova Scotia*. PhD thesis, Dalhousie University, Halifax, 426 pp.

WIGHTMAN, D.M. & COOKE, H.B.S. (1978) Postglacial emergence in Atlantic Canada. *Geosci. Canada*, **5**, 61–65.

WILLIAMS, H. (1979) Appalachian orogen in Canada. *Can. J. Earth Sci.*, **16**, 792–807.

WOODROFFE, C.D., CHAPPELL, J.M.A., THOM, B.G. & WALLENSKY, E. (1985a) Geomorphology of the South Alligator tidal river and plains, Northern Territory. In: *Coasts and Tidal Wetlands of the Australia Monsoon Region* (Ed. by K. N. Bardsley, J. D. S. Davie & C. D. Woodroffe), pp. 3–15. NARU Monograph, ANU Press, Canberra, 190 pp.

WOODROFFE, C.D., CHAPPELL, J.M.A., THOM, B.G. & WALLENSKY, E. (1985b) Stratigraphy of the South Alligator tidal river and plains, Northern Territory. In: *Coasts and Tidal Wetlands of the Australia Monsoon Region* (Ed. by K. N. Bardsley, J. D. S. Davie & C. D. Woodroffe), pp. 17–30. NARU Monograph, ANU Press, Canberra, 190 pp.

WOODROFFE, C.D., CHAPPELL, J., THOM, B.G. & WALLENSKY, E. (1989) Depositional model of a macrotidal estuary and flood plain, South Alligator River, Northern Australia. *Sedimentology*, **36**, 737–756.

WRIGHT, L.D., COLEMAN, J.M. & THOM, B.G. (1973) Processes of channel development in a high-tide-range environment: Cambridge Gulf–Ord River Delta, Western Australia. *J. Geol.*, **81**, 15–41.

WRIGHT, L.D., COLEMAN, J.M. & THOM, B.G. (1975) Sediment transport and dispersion in a macrotidal river channel, Ord River, Western Australia. In: *Estuarine Research* (Ed. by L. E. Cronin), II, pp. 309–321. Academic Press, New York, 587 pp.

YEO, R.K. & RISK, M.J. (1981) The sedimentology, strati-

graphy, and preservation of intertidal deposits in the Minas Basin system, Bay of Fundy. *J. sedim. Petrol.*, **51**, 245–260.

ZAITLIN, B.A. (1987) *Sedimentology of the Cobequid Bay–Salmon River estuary, Bay of Fundy, Canada.* PhD thesis, Queen's University, Kingston, 391 pp.

ZAITLIN, B.A. & DALRYMPLE, R.W. (1985a) Depositional patterns and stratigraphic sequences from the inner part of A sand-dominated, macrotidal estuary, Cobequid Bay–Salmon River estuary, Bay of Fundy. *Abstrs Int. Ass. Sedimentol., Symp. Modern and Ancient Clastic Tidal Deposits, Utrecht*, 169–172.

ZAITLIN, B.A. & DALRYMPLE, R.W. (1985b) Depositional controls on facies zonation in sandy, macrotidal estuaries: a conceptual model from the Cobequid Bay–Salmon River estuary, Canada. *Geol. Soc. Am. Abstr. with Progr.*, **17**, 759.

(Manuscript received 1 March 1989; revision received 28 December 1989)